MEASUREMENT OF THERMAL CONDUCTIVITY OF AQUEOUS ORGANIC LIQUIDS USING THE RELATIVE TRANSIENT HOT-WIRE TECHNIQUE

By

EDWARD RYAN PETERSON

Bachelor of Science
Houghton College
Houghton, New York
1974

Master of Science
Rice University
Houston, Texas
1981

Submitted to the Faculty of the
Graduate College of the
Oklahoma State University
in partial fulfillment of
the requirements for
the degree of
DOCTOR OF PHILOSOPHY
May, 1985

Thesis
1985D
P485m
cop.2

OKLAHOMA STATE
UNIVERSITY
LIBRARY

MEASUREMENT OF THERMAL CONDUCTIVITY OF AQUEOUS ORGANIC LIQUIDS USING THE RELATIVE TRANSIENT HOT-WIRE TECHNIQUE

Thesis Approved:

R. N. Maddox
Thesis Advisor

Morris

Kenneth J. Bell

Anthony L. Hines

Norman N. Durham
Dean of the Graduate College

1238353

PREFACE

A relative hot-wire apparatus for measuring thermal conductivity of electrically non-conductive liquids was modified for measuring electrically conductive liquids and a new hot-wire design was developed. The accepted measurement method was corrected to eliminate the effect of thermal diffusivity upon the measurement. Contrary to accepted theory, the measurement can depend upon the reference fluid used. Several modifications to the apparatus were made to improve the accuracy and reproducibility of the measurements. To prove the method and apparatus, the thermal conductivity of aqueous solutions of formic, acetic, propionic, and n-butanoic acids were measured from 70 to 350 F. Reasonable to good agreement with published data was obtained.

I wish to thank Dr. Robert N. Maddox for his guidance and encouragement during the course of this work. I also wish to express my gratitude to Dr. G. J. Mains, Dr. K. J. Bell, and Dr. A.L. Hines for their willingness to serve as members on my advisory committee. My appreciation goes to Mr. Ross Fox for his technical assistance and many helpful suggestions.

I would like to recognize the financial support Phillips Petroleum provided me throughout my course of study at Oklahoma State University.

My wife, Janet, receives my deepest thanks for her continued patience, support, understanding, and encouragement.

TABLE OF CONTENTS

LIST OF TABLES

LIST OF FIGURES

LIST OF SYMBOLS

A	area
A_x,A_y	resistance temperature coefficient
a	filament radius
Btu	British Thermal Unit
b	unknown real number
C	degrees centigrade
C_N	unknown constant
C_o	thermal conductivity calibration constant
C_p	heat capacity at constant pressure
C_v	heat capacity at constant volume
C_x	pseudo-constant
C^*	Euler's constant, approximately 1.781
cm	centimeter
d	differential operator
E_t	pen deflection per unit temperature change
E_v	recorder sensitivity
e,exp	exponential operator
F	degrees Fahrenheit
G_x,G_y	differential amplifier gain
g	denotes ethylene glycol as subscript
gm	gram mass
I_0,I_1	Bessel function

i	index integer or complex part of a number
J_0, J_1	Bessel function
j	index integer
K	degrees kelvin
K_0, K_1	Bessel function
kl	unknown real number
l	length
ln	natural logarithm
m	mass fraction, meter
mm	millimeter
N	mol fraction
n	any integer
Q,q	heat flux
Q_{el}	electrical heating
Q_{rad}	heat transfer via radiation
R_r	reference cell electrical resistance
R_s	resistance temperature coefficient
R_t	test cell electrical resistance
r	radius or radial direction
r_o	filament radius
r_i	radius of insulated filament
T	temperature
T_L	liquid temperature
T_W	wall temperature
t	time
W	watt
w	weight fraction, denotes water if subscript

wt	weight
V	volume fraction, voltage
V_{br}	bridge voltage
V_r	reference cell voltage
V_t	test cell voltage
Y_0, Y_1	Bessel function
#	pound mass
%	percent
α	thermal diffusivity
Δ	change (in)
γ	natural logarithm of Euler's constant, approximately 0.5772
λ	thermal conductivity
μ	variable real number
π	approximately 3.14159
ρ	density
σ	Stefan-Boltzmann constant
θ	slope or angle
δ	partial differential operator
∞	infinity
$L\{\ \}$	LaPlacian operator
$\bar{t}$	LaPlace transform of temperature
Γ	product operator
Σ	sum operator

CHAPTER I

INTRODUCTION

Liquid thermal conductivity is a vital property for engineering design and basic heat transfer studies, but can be difficult to measure accurately. Data accurate to within five percent are acceptable, and most accurate data has been obtained only within the last thirty years. Except for a very few common liquids, thermal conductivity data are only available in a limited temperature range, usually 20 to 30 C. Very little data exist for mixtures, most of which do not include water.

The original intent of this study was to create an apparatus capable of measuring thermal conductivity of electrically conductive liquids for a wide temperature range based on the relative hot wire design. The data of several solution types would then be correlated by a group contribution method.

After the modified probe was made, thermal conductivity measurements were taken according to accepted practice and theory. For all fluids, data were consistently low or high. Subsequent investigation of the measurement method revealed that it was based on an incorrect mathematical model, which contained an incorrect simplifying assumption. The mathematical model was correctly re-derived. The measurement method was altered based on the corrected mathematical model, and better data were obtained. Modifications were made to the apparatus to improve the accuracy and reproducibility of the measurements.

The apparatus was tested by measuring the thermal conductivity of several organic acids and their solutions. The final measurements were reproducible and agreed well with published data.

CHAPTER II

LITERATURE SURVEY - MEASUREMENT METHODS

The property of a liquid to transfer heat by conduction alone is difficult to measure because liquids are easily subject to convection. Even very carefully designed experiments can give highly inaccurate measurements of liquid thermal conductivity due to the rapid onset of convection. Thermal conductivity experiments which are allowed to come to equilibrium often unintentionally include some convective heat transfer. Measurements made before thermal equilibrium is attained can be difficult to model mathematically. Transient equations include the additional factor known as thermal diffusivity.

Recent advances in electronics and manufacturing have made many of these problems less acute. Temperature, absolute heat transfer, absolute resistance, electrical potential, etc., can now be measured accurately. The equipment used to take measurements, such as thermocouples or calibrated resistance wires, can be made small, so that the measurement probe does not interfere in the measurement itself. More accurate machining and measuring devices reduce systematic error in experiments which require manufacture to exacting tolerances.

Despite the growing sophistication of thermal conductivity devices, the amount of new thermal conductivity data has not grown appreciably. Many recent publications are more accurate evaluations of liquids measured before. Most of the reported data covers a limited temperature range. Limited data is the result of the difficulty of building and operating most thermal conductivity measurement equipment. Many devices require several hours to reach equilibrium so that data may be taken.

There are only a few good, basic designs for the devices which measure thermal conductivity. This survey will explain how these devices work, as well as discuss each type through representative examples.

Basic Thermal Conductivity Probes

Tye (75) and Tsederburg (78) give excellent reviews of the methods of thermal conductivity measurement and representative results obtained to 1969. Jameison et al (35) give an exhaustive review of the available liquid thermal conductivity data to 1973. These surveys, which include the results of hundreds of authors, reveal that only two basic design types are used with regularity. They are the hot-wire, and the parallel surface. The reason for this is the simpler the design, the more exactly the design can be modelled mathematically. More recently, a few additional methods have been developed for liquid thermal conductivity measurement. The thermal comparator, originally designed for measuring thermal conductivity of solids, is discussed for use with liquids later in this chapter. Optical methods relate the change in refractive index, due to a temperature rise, to the thermal conductivity.

The Parallel Surface

This method utilizes three simple geometries: the plane surface, the cylinder, and the sphere. Each will be discussed.

The Horizontal Flat Plate

Horizontal plates are modeled mathematically by infinite, parallel, plane surfaces. The mathematical representation of this geometry is:

$$\lambda = ql/[A(T_1 - T_2)] \tag{2.1}$$

Normally, two identical metal plates, having both a length and width much greater than the uniform gap between them, are maintained at different temperatures. The liquid to be measured is inserted between the plates. The top plate is generally the warmer so that convection is minimized. The plates are commonly made from good conducting materials, such as copper, silver, gold, aluminum, or chromium, with compensating heaters or insulating seals at the edges. Polished metal surfaces, with low emissivities, reduce radiant heat transfer. The temperature of the plates is measured as close as possible to the liquid face of the plate using imbedded thermocouples.

The problems with this method include: convective currents, especially at the edges; optimizing the thinness of the liquid layer against irregularities in the plate surfaces and the gap between them; and maintaining isothermal conditions at the plate surface for times long enough to establish thermal equilibrium.

Measurements often take several hours. Many measurements are usually required for one material at one temperature to insure convection is not present. Secondary heat flows, due to the large mass of the measurement cell, are often larger than the primary flow of heat across the liquid layer. High pressure measurements are usually poor, since the plates must be made thicker and the equipment bulkier to maintain a uniform gap. For near-critical fluids, this method is best, as the density gradient as a function of temperature is large.

Amirkhanov et al (5) recently used the flat plate method to make absolute measurements of the thermal conductivity of water as a function of pressure and temperature to the critical point. The heat flow through the device was monitored by a compensation furnace at the plate edges and precision calibrated thermocouples couples situated in the plates. The compensation heater maintained the plate edges at the mean temperature of the plates. Corrections for secondary heat flow were calculated using precise thermal conductivity data for the metal plates and pressure containment block, all made from the same steel alloy. Corrections also included plate area changes due to thermal expansion. Measurements of the plate separation distance were claimed precise to 0.001 mm (0.33%) and the plate area to 0.03%. The heat supplied at the upper plate was known to within 0.13%. The reported maximum measurement error was 2%.

Instead of a compensation heater at the plate edges, Gurenkova et al (26) employed fluoroplastic seals, having a lower thermal conductivity than the liquids measured, to reduce secondary heat flows and convection at the plate edges. Small sections of optical glass were substituted for fluoroplastic at opposite ends of the cell so that interferograms could be made of the liquid at steady state. Temperature differences were measured from the interferograms. The device was standardized using a metal plate of known thermal conductivity. By using a relative device instead of an absolute device, the authors escaped making exacting measurements of the dimension of their cell and corrections for secondary heating. Gurenkova et al (26) made measurements at room temperature only, because the plastic insulator would distort at high temperatures.

Ogiwara et al (57) used glass plates instead of metal plates for their study of pure, normal alcohols. Instead of measuring absolute thermal conductivity, they calibrated their cell with water. Large water baths of different temperatures kept each plate at their respective bath temperatures. Bath temperatures were maintained within 0.01 C. Reported accuracy was ±3%, although results were usually 4 to 8% lower than reported elsewhere in the literature. Although of questionable accuracy, and only good at low pressures, the equipment was reportedly easy to build and operate.

Vertical Coaxial Cylinders

Vertical coaxial cylinders of small clearance are represented mathematically as infinite, parallel surfaces. The solution to the heat conduction equation is;

$$\lambda = q\ (\ln(r_2/r_1))/[2\pi\ell(T_1 - T_2)] \qquad (2.2)$$

A thin film of liquid in the annulus between the two cylinders is heated by the inner cylinder. The greater the length to diameter ratio, the better the mathematical model depicts the actual device. Insulators or compensatory heaters are required at the ends of the cylinders. Due to the system geometry, the end area is relatively less than in the flat plate method, reducing the problem of secondary heat flows.

Additionally, cylindrical surfaces can be machined to better tolerances than flat surfaces, and the separation distance is usually more uniform. Because the concentric cylinder device has fewer sources of error, it is generally preferred over the flat plate method. Less distortion in the wall separation will result at high pressure and temperature, and the mass of the system can be less at comparable pressures. The problems with convection are nearly the same as with the flat plate.

Le Niendre et al (44) employed a concentric cylinder apparatus to measure the thermal conductivity of normal and heavy water over a wide range of temperature and pressure. The inside of the inner cylinder and outside of the outer cylinder were insulated with sintered alumina. Centering pins were also made of sintered alumina. Eight thermocouples equally spaced along the cylinder walls at the alumina interface were used to measure the temperature difference between the cylinder walls. A platinum-rhodium wire was used to supply a known amount of heat to the inner cylinder wall, based upon a known applied current. Secondary heat transfer was removed as a factor through calibration with helium at high pressure. All surfaces in contact with the water were platinum-rhodium alloy. The expansion coefficient and thermal conductivity of this material was well known. The cylindrical surfaces were polished to a high brilliance after machining. Total reported error was 1.5% up to 350 C.

Although normally a steady-state device, the concentric cylinder apparatus can be operated in an un-steady state mode. An example of this is the "regular regime" method developed by Golubev (23). The heat capacity of the fluid, as well as heat capacities and thermal conductivities of all the materials in the cell, had to be known to make determinations of fluid thermal conductivity. Guard heaters at each end corrected for secondary heat losses. The internal cylinder was heated 1 to 6 C above the external cylinder. After steady state was reached, the heater in the internal cylinder was turned off. The initial cooling rate of the inner cylinder was related to the thermal conductivity of the fluid in the annulus.

Concentric Spheres

The solution of the conduction equation for concentric spheres is:

$$\lambda = q(r_2 - r_1)/[4\pi r_2 r_1 (T_1 - T_2)] \qquad (2.3)$$

The thin film between the spheres is heated by the inner sphere. Temperature probes enter the inner sphere through alignment plates, which maintain concentricity of the spheres. There is no problem with modeling this system mathematically, but the practical problems of constructing and using this method ensure it is not used often. Keeping the gap uniform around the entire surface is difficult, as is keeping the fluid in the gap at high pressures.

Schrock and Starkman (68) built a spherical cell for measuring the thermal conductivity of viscous liquids. The inner and outer spheres were made of copper, with a 25 mm gap between them. A smaller gap is not practical because this device is especially difficult to center, yet very sensitive to gap width variations. An accuracy of 2% was reported for the viscous oils that were measured. This device is not recommended for measuring the thermal conductivity of light, low viscosity hydrocarbons because the large gap would allow significant convection to occur.

The Hot Wire

The hot-wire is mathematically similar to the concentric cylinder method. (The wire serves as the central cylinder, the fluid being heated by the wire) The wire can also act as a thermometer. (The external cylinder, when present, is often glass or quartz. The temperature of the external cylinder is usually measured with a resistance thermometer or a series of thermocouples. Alternatively, a platinum tube can serve both as an external cylinder and a resistance thermometer).

The hot-wire device is easier to build than any of the parallel surface methods. (Secondary heat flow is reduced, as the equipment is much less massive. There are no complicated routes for heat to flow out of the measurement area. When used as a steady state, absolute measurement device, the diameter of the wire and external tube must be known exactly, and the wire must be aligned to be perfectly coaxial with the outer cylinder.

The hot-wire method is generally preferred in recent years due to readily available wire filament of small diameter and sophisticated yet inexpensive electronics. The small mass of the cell allows for rapid attainment of thermal equilibrium, and relatively thin walls for high pressure work.

Nietro de Castro et al (54) describe an absolute apparatus using two fixed platinum wires. Each thin wire is made one arm of an automatic Wheatstone bridge. Calibrated resistance switches accurately detect increases in resistance during the measurement, triggering timers. No external cylinder is necessary, as steady-state is never reached. The measurement time is approximately two seconds. Two wires of different length with duplicate connections are used to cancel out filament-to-support wire connection effects, also known as end effects, as the resistance change in the shorter wire is subtracted from that of the longer wire. The cell containing the wire is made of steel for high pressure work. Thermal equilibrium is achieved when the wire resistance remains constant with time.

In a more recent paper (55), Nietro de Castro et al improved the accuracy and speed of the electronic switches. The filament was still fixed at the upper end, but the lower end was connected to a small platinum weight to keep the wire taut and eliminate strain effects. The platinum weight was connected to the electronics system with a thin piece of gold tape.

(The hot-wire method is often used as a relative device. The cell is calibrated using a fluid of known (or accepted) thermal conductivity. Calibration effectively eliminates the need to know the cell dimensions exactly, and the need for an external cylinder in some instances, and includes systematic heat losses in the calibration factor).

Raal et al (62) also used a two wire system to eliminate end effects, and a tiny stainless steel spring to keep tension on the wire, as a weighted filament may move during the experiment. Multipole gold switches and connections were used to reduce contact resistances in the timing and resistance measurement switches. The cell was standardized with ethylene glycol both to eliminate the effect of convection during calibration and because its thermal conductivity was close to that of the normal alcohols measured.

Bare wire, heated by direct current, precludes the measurement of electrically conductive liquids. Several authors have coated the thin filament to measure such liquids while using direct current heating.

Nagasaka and Nagashima (52) coated a platinum filament with a thin polyester coating nearly one-fifth the wire diameter. The two wire method was used. The filament supports were coated more thickly with a silicone rubber. Instead of switches, which have inherent time lags, a bridge circuit was used to convert the bridge resistance change to a voltage measurement as a function of time. The reported upper temperature limit on this polyester coated wire was 150 C, although the authors did not report data above 50 C.

Alloush et al (4) improved the coated wire technique by anodically oxidizing a tantalum filament. The coating thickness was reduced to less than 1% of the filament diameter, and the coating thickness was made uniform. Tantalum oxide is a strong, adherent coating and may be useful up to 200 C as an electrical insulator when in contact with electrolyte solutions (51). However, the support wires were still coated with silicone rubber for electrical insulation. To eliminate strain, a gold spring was used to adjust and fix the wire tension. Reported accuracy was 3%, and the useful temperature range was 20 to 80 C, limited by the silicone rubber used on the support wires.

An alternative to coating the wire for measuring electrically conductive liquids is to employ alternating instead of direct current to heat the wire. Irving and Jameison (33) designed such a device. The frequency of the system was optimized at 1000 Hz, reducing both interference from external electrical sources and capacitance effects. The simplicity of the method was offset by the cost of the special electrical equipment, which included a null detector, voltmeter, bridge, and voltage divider designed specifically for use with alternating current. Alternating current methods are difficult to adapt to transient measurement, so the steady-state method was used. One measurement was taken per hour, but measurements at eight different power settings were needed to establish a linear relationship between wire resistance and power input. Reported accuracy was 3%.

Phylippov et al (59) constructed a device to measure thermal conductivity, thermal diffusivity, and volumetric heat capacity simultaneously. Platinum foil was used instead of wire. Thermophysical properties were related to the thermal oscillations in the probe due to induced changes in the electrical phase and frequency of 10 to 100 Hz. Reported accuracy was better than 1.5% over a temperature range of 300 to 600 K. Due to the nature of polar and electrically conductive molecules to flip or "ring" at such low frequencies, in harmony with the electrical phase, such materials could not be measured.

Optical Methods

These methods are relatively new. Optical methods generally involve measuring a change in index of refraction as a function of fluid temperature (12,13,14,20,22,24,31,38, 40,43,71,73,74). Lasers can be used to heat the liquid and also measure the change in refraction index. As the laser light passes through the medium, some of the energy is absorbed by the fluid and converted into heat. As the liquid warms, its index of refraction is changed. The change in path of the laser beam is measured and related to the liquid thermal conductivity. Also, the cylindrically heated sample can act as a lens, and a change in focal length is related to a change in thermal conductivity. Unfortunately, both methods actually measure thermal diffusivity, so the heat capacity, index of refraction, density, and absorption coefficient, all as a function of temperature, must be known before thermal conductivity can be calculated. Claimed accuracy varies from 15 to 25% (31,73) to as good as 6% (38). This method is not the most accurate of those given. Its most important use is for investigating small amounts of materials, local properties of nonhomogeneous materials, and fluids near their surfaces or critical point. Optical methods can be designed to be non-intrusive and measure properties of very small regions.

Thermal Comparator

This is a relative method for obtaining thermal conductivity over a limited temperature and pressure range. The device is a block of insulating material containing small metal balls containing thermocouples linked to read differential temperature. Powell and Groot (61) have used a thermal comparator to measure the thermal conductivity of several alcohols, organic acids, and hydrocarbons at 30 C. Initially, the comparator block was cooled to 14 C. One metal ball was brought into contact with a taut membrane covering the test liquid, while the other was suspended above the liquid. The difference in electromotive potential of the thermocouples was recorded as a function of time. The initial slope of increasing electromotive force was related directly to the thermal conductivity. Accuracies were reported to be within 4%.

Not useful at high temperatures, the apparatus is simple to build, use, and operate, while giving limited information on the thermal conductivity of materials. Using this non-intrusive method, the apparent thermal conductivity of materials such as living animal tissue, vegetable tissue, and animal decay products can be measured.

CHAPTER III

LITERATURE SURVEY - AQUEOUS SOLUTIONS

Very little data have been compiled to date on the thermal conductivity of aqueous solutions of organic compounds. Jameison et al (35) list data for only 18 aqueous solutions, including only alcohols, amides, acids, and glycols. Aqueous formic, acetic, and n-butanoic acid data are reported by Usmanov (35) at 20 C. Lees (35) reports three aqueous acetic acid data points at 11 C. A search of the published literature has revealed no further data on aqueous organic acid solutions, although more work has been done on other aqueous organic solutions (6,10,36,63,81). The need for aqueous data over a wide temperature range is clear. The measurement of aqueous organic acids presents a particular problem due to their high electrical conductivity and corrosiveness. Formic acid is almost as good an oxidant as sulfuric acid (37). At temperatures in excess of 100 C, all of the acids in this work attack stainless steel.

CHAPTER IV

LITERATURE SURVEY - PREDICTIVE EQUATIONS

Several equations have been proposed for fitting and/or predicting thermal conductivity of liquids as a function of temperature and/or composition. Thermal conductivity for most pure non-metallic liquids decreases linearly with increasing temperature. Notable exceptions to this are water (1), sulfur (35), phosphoric acid (35), and most diols, triols, and glycols (35). Water shows a strong maximum in thermal conductivity between 250 and 300 F. Sulfur, phosphoric acid, and most diols, triols, and glycols show a near linear increase in thermal conductivity with an increase in temperature at low temperatures.

Except for water, most pure liquid data can be represented by linear or quadratic equations. There is severe dispute as to which mixing rule is best for non-aqueous mixtures. Very few correlations exist for representing the thermal conductivity of aqueous solutions.

Grishchenko et al (25) proposed a simple non-linear equation for several aqueous solutions.

$$\lambda = \lambda_1 m_1 + \lambda_2 (1 - m_1)^2 + \lambda_0 m_1 (1 - m_1) \qquad (4.1)$$

The subscript (1) refers to the non-aqueous component. The factor λ_o refers to the effective thermal conductivity of water in a solution when not present. Modest success was achieved for the ten solutions evaluated. All data was for 30 C only and only binary mixtures.

Usmanov (81) proposed a similar model.

$$\lambda = \lambda_1 m_1 + \lambda_2 m_2 - \alpha m_1 m_2 \qquad (4.2)$$

In this case, α is a fitting factor. Deviations of no more than 3% were attained with this equation for five binary solutions at 30 C.

Rastoguev and Ganiev (63) proposed a much more complicated model:

$$\lambda = \{\lambda_2 N_2 + \lambda_1 R\}/(N_2 + R) \qquad (4.3a)$$

$$R = 2N_1 \, [(V_1/V_2) - 1] \qquad (4.3b)$$

with N and V representing mol fraction and mol volume of the respective components. Ten to fifteen percent error is common using this equation, and the predicted value is always less than that measured.

Li (45) has proposed a method without empirical fitting factors based on the harmonic mean of the molar volumes. Of the models discussed here, this is the only one which can be used with mixtures of more than two components.

$$\lambda = \Sigma_j \Sigma_i \phi_i \phi_j \lambda_{ij} \tag{4.4a}$$

$$\lambda_{ij} = 2[1/\lambda_i + 1/\lambda_j] \tag{4.4b}$$

$$\phi_i = m_i V_i / \Sigma_j m_j V_j \tag{4.4c}$$

$$\Sigma_i \phi_i = 1 \tag{4.4d}$$

Errors are generally less than 3% at 40 C. Use of the geometric mean

$$\lambda_{ij} = (\lambda_i \lambda_j)^{1/2} \tag{4.4e}$$

yields an average absolute error near 5%, while the arithmetic mean

$$\lambda_{ij} = (\lambda_i + \lambda_j)/2 \tag{4.4f}$$

yields an average absolute error near 12%.

Jameison and Hastings (34) proposed a relation based upon the weight fraction of the mixture components.

$$\lambda = \lambda_1 w_1 + \lambda_2 w_2 - \alpha | \lambda_2 - \lambda_1 | (1 - w_2^{1/2}) w_2 \tag{4.5}$$

which gives deviations from experimental values under 4% for more than 90% of the data for the 20 mixtures investigated.

Bohne et al (10) recently measured the thermal conductivity of ethylene glycol and water and glycol-water solutions from -20 to 180 C. Using a slight modification of the Filippov equation, they fit their data with an accuracy of ±1%. Their equations for water and ethylene glycol in this range are:

$$\lambda_w = 0.56276 + 1.874 * 10^{-3}T - 6.8 * 10^{-6}T^2 \quad (4.6a)$$

$$\lambda_g = 0.24511 + 1.755 * 10^{-4}T - 8.52 * 10^{-7}T^2 \quad (4.6b)$$

The Filippov equation as modified by Bohne et al is:

$$\lambda = \lambda_w(1 - w_g) + w_g\lambda_g - Z(\lambda_w - \lambda_g)(1 - w_g)w_g \quad (4.6c)$$

where the pseudo-constant (z) is:

$$Z = 0.6635 - 0.3698 * w_g - 8.85 * 10^{-4}\ T \quad (4.6d)$$

Thermal conductivity is given in W/mK, the subscript g refers to glycol, and the subscript w refers to water.

These equations for thermal conductivity are empirical. Several authors have attempted to develop theoretically based equations for thermal conductivity, but invariably use one or more empirical fitting factors to obtain useful results.

Ogiwara et al (57) attempted to model a pure fluid as a quasi-lattice, and used the Lennard-Jones potential function to model interactions between molecules. Besides including heat capacity, Stiel's polar factor, and Pitzer's acentric factor in the equation, four empirical constants appeared. These constants were obtained by fitting to experimental data. The model was useless for predicting general liquid thermal conductivity. The error averaged 3% for the ten alcohols measured.

Saksena and Harminder (65,66) attempted to include self-diffusion factors into a predictive equation for mixtures without using an empirical fitting constant, although retaining the pure component thermal conductivities as factors. However, they related the self-diffusion coefficient to molar volume and mol fraction. In their first paper, the final equation included only mol fraction, molar volume, and pure component thermal conductivity as factors. The average error is about 7%. In their subsequent paper, they introduce two empirical coefficients into their first equation in order to reduce their average error for mixtures to 2.5%. All fitted data were at 0 C. No mixtures contained water.

Baroncini et al (8) discussed various semi-empirical methods proposed by other authors for predicting pure liquid thermal conductivity. Their improved equation included only molecular weight, molar volume and heat of vaporization at the normal boiling point, and reduced temperature, besides one fitting factor per compound. Their results for 20 pure liquids for T_r from 0.3 to 0.7 give an average deviation of only 1.1%. Water was not included in their list, and none of the components in the list increased in thermal conductivity with increasing temperature. The end result was good but not amazing. As the normal boiling point and molecular weight were constants, these values could have been incorporated into the constant term. The equation reduces to simply a single function of temperature. The temperature functionality is nearly linear, which is a standard way to represent thermal conductivity of most liquids.

Allen (3) and Scripov (72) discuss why theory for liquids is inadequate for calcula explaining the mechanism of thermal conduction in liquids or predicting good values of thermal conductivity. Allen indicates that heat in nonmetallic solids is transferred by lattice-type vibrations. The more perfect the crystalline structure of the solid, the better theory can predict the rate of the heat transfer process. However, even a few structural imperfections reduce the accuracy of the prediction. Liquids have too many structural imperfections for the solid model to be applied, but are so densely packed that the gaseous model is less accurate. The theory of thermal conductivity for glasses is in its infancy, from which may eventually come a theory for normal liquids. Scripov states: " There is yet no exhaustive answer to how a liquid is constructed. A liquid, as a dense, irregular structure, is more unique than assumed by quasi-crystalline representations. It is characterized by more numerous and "free" local configurations than an ordered regular structure. The high mobility of the particles and the presence of small groups of particles (with a density exceeding the crystal density) create favourable conditions for the exchange of energy and molecular arrangements. "

CHAPTER V

METHOD DEVELOPMENT

Of the methods discussed in Chapter II, the insulated transient hot-wire method is the most attractive for measuring thermal conductivities of electrically conductive solutions over a wide temperature range.

The parallel surface methods are subject to convection, require several hours to days for each data point, are costly to build, and are subject to severe secondary heat flow. The thermal comparator is only useful over a limited range of pressure and temperature. Optical methods are very expensive because they require lasers and laser optics systems. The accuracy of such systems is often poor. The alternating current hot-wire, although less expensive and difficult to construct than the parallel surface methods, is still much more costly than the simple direct current insulated hot-wire.

Alloush et al (4) presented a good method for creating an insulated filament. Instead of attempting to place a polymeric coating on a platimum filament, they used a tantalum filament and anodically oxidized the filament surface. The oxide coat was uniform, extremely thin, and resistant to chemical attack, as well as a good electrical insulator. Thereby, they were able to measure the thermal conductivity of salt solutions, relative to water, from 20 to 80 C. Their support wire was insulated with silicone rubber, however, which limited the temperature of his measurements. Additionally, any fluid which could chemically attack the silicone rubber could not be measured by Alloush et al.

The Modified Method

The method presented by Alloush et al (4) was modified to allow measurement of corrosive solutions and increase the useful temperature range. Primarily, the support wire coating had to be changed to a more durable material. By making the support wire out of the same pure tantalum as the filament, its surface was coated with tantalum oxide at the same time as the filament surface. Tantalum oxide is resistant to corrosive attack at high temperatures, making it an ideal insulator on both the filament and support wire. The silicone rubber use by Alloush et al (4) could peel away from the support wire, especially around the filament. The continuous, all-tantalum oxide coating did not have this problem.

Alloush et al (4) soldered the tantalum filament to support wires made of different metals: one was copper, the other platinum. Soldering was done at temperatures in excess of 700 C, in an oxygen free atmosphere, using a gold-silver alloy solder. The support wires were subsequently coated with a silicone rubber. Then the filament was oxidized. In this work, the tantalum filament was connected to a tantalum support wire by cold-welding. The filament and support wire were oxidized as a unit. No special materials, equipment, or conditions were necessary for cold-welding. The cold welding equipment used in this work included: a bench vise, stainless steel pressing blocks, and a steel file.

To make the weld, a small slot was filed in the soft tantalum support wire at an end. The filament was set between the sides of the slot, and the support wire was welded on the filament. Because the support wire itself was 0.035 inches in diameter, and the welded section of the support wire was about 0.2 inches long, approximately 2 million pounds per square inch was applied at the weld site. A strong weld was formed.

After the filament and support wire were welded, the unit was cleaned in an acid bath containing only fuming sulfuric, concentrated hydrochloric, and hydrofluoric acid. The cleaning process required 30 seconds to one minute, as the acid mixture was strong, and quickly removed any organic or inorganic film on the metal surface. The unit was then rinsed in boiling distilled water for 10 to 20 minutes, to remove any tantalum fluoride film that may have formed on the wire surface during cleaning. The unit was then immersed in a 0.2 molar sulfuric acid cell. A piece of platinum wire was used as the cathode. A current density of approximately one milliamp per square centimeter was maintained on the tantalum unit. The oxidation required approximately 12 to 24 hours. When complete, the oxide coating gave the filament and support system an apparent resistance in excess of 3 mega-ohms while in the sulfuric acid solution.

The support wire was conveniently oxidized along with the filament. There was no need to coat it otherwise. The oxide coating was uniform and continuous over the entire surface (4). Because the oxide coating was only two microns thick, it did not flake (79). Additionally, tantalum oxide is electrically one of the best insulators and crack resistant metal oxides known (79). The oxidized filament wire was useful as an insulator in contact with electrically conductive fluids up to 200 C (50).

Once the tantalum unit was oxidized, it was secured into the pressure bomb top, shown in Figure 1, using special heat resistant, pressure molded seals. Each support wire was cold welded to copper wire for connection to a low resistance gold-plated multi-pin connector which led to the electronic apparatus.

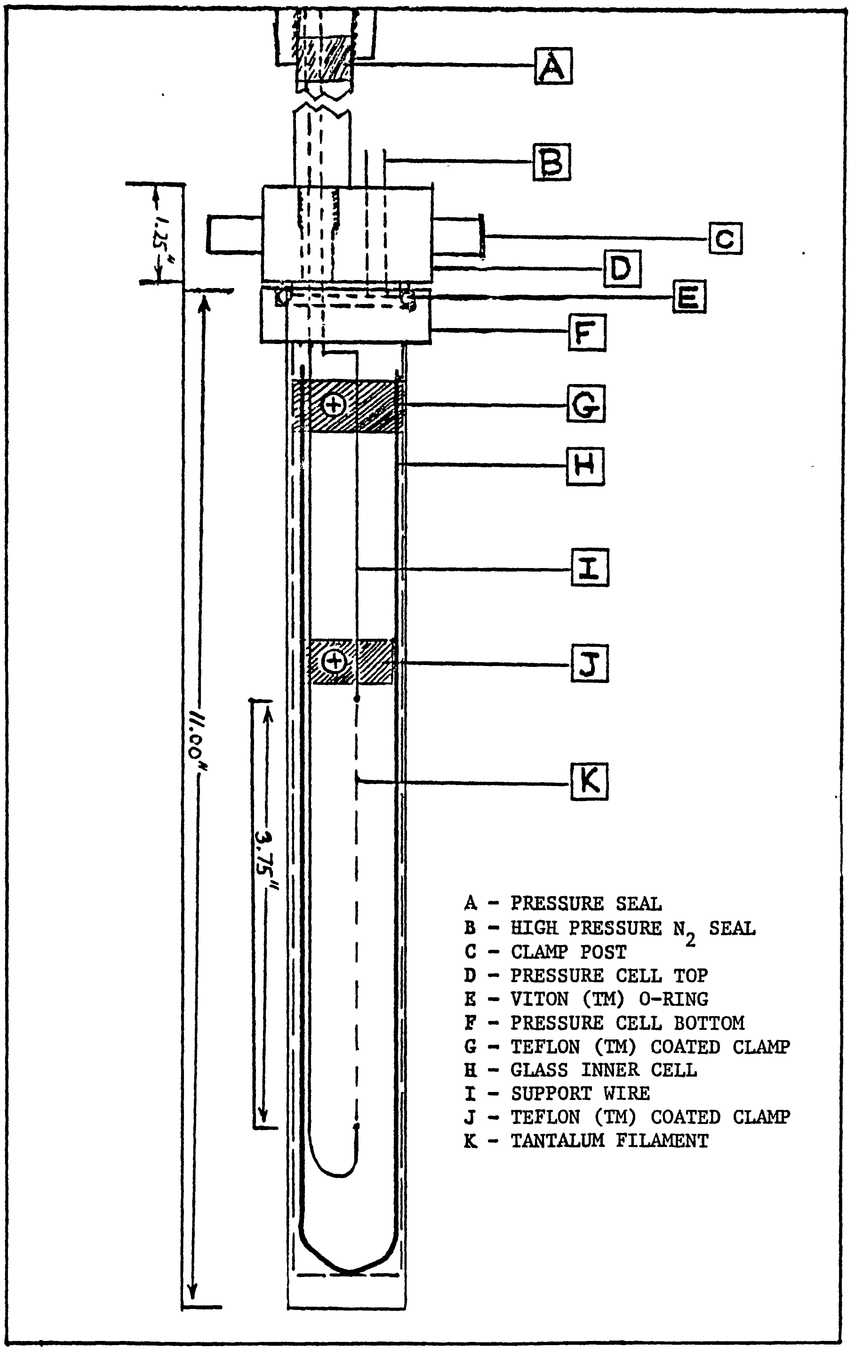

Figure 1. Thermal Conductivity Cell

Further Modifications

The hot-wire method requires that the filament be maintained straight and taut between the support wire. At first, the support wire was fixed at the top and bottom of a glass tube with Kovar seals, based on the design of Nangia and Chenoweth (53). When the Kovar glass seal was melted around the tantalum wire, then allowed to cool, the Kovar seal cracked because the thermal expansion coefficient of tantalum is smaller than that of most metals compatible for use with Kovar glass seals. Since the support wire could not be fixed in either end of the glass tube, the support wire was shaped, as is shown in Figure 1, and held rigid by Teflon coated clamps in an open tube. The support wire was oxidized above the point of the Teflon pressure seal. This design had several advantages. First, the oxidized support wire was never subject to temperatures required to melt the Kovar or any glass seal, which could have reduced the oxide coating. Second, the filament could be relaxed and somewhat coiled during cold welding, but drawn straight and taut, using the clamps, before oxidation and measurement. Making the filament to an exact length was simplified, and the unstressed delicate filament did not break during cold welding.

During initial tests, the smooth glass walls of the tube containing the liquid often scratched the thin oxide coating on the support wires when the wire unit was immersed in the liquid. To prevent this, a slot was cut in the glass tube at the top and the clamps were wrapped with Teflon tape so the bottom clamp would just slide into the tube, and the top clamp fit securely into the slot and between the metal walls of the pressure cell. During immersion of the wire, the bottom support guided the filament into the cell. The top and bottom clamps held the wire unit firmly in the center of the glass tube. The top clamp held the glass tube firmly in the center of the metal tube. Between the top clamp and the pressure seal, Teflon tubing was slipped over each end of the oxidized support wire to ensure the support wire would not be scratched by contact with metal and cause an electrical short.

The final design, shown in Figure 1, required no soldering, special handling, or tension springs. It was not subject to thermal strain along its axis because it was made of only one material and only the top was fixed. The oxide coating was easy to apply, thin, and continuous. The tantalum filament was run through approximately 50 temperature cycles between 70 and 400 F to test the integrity of the cold welds and determine if the tantalum wire filament would experience a resistance change with temperature cycling. The cold welded joints proved strong and no resistance change in the filament was measured. The sample tube was easy to fill and clean, since it was not connected to the wire unit. The useful temperature range was increased to 150 - 175 C. Finally, highly corrosive, electrically conductive materials (i.e. aqueous formic and acetic acid) could be measured since the fluid contacted only Teflon or tantalum oxide.

CHAPTER VI

CHOICE OF MEASUREMENT TIME AND CALIBRATION LIQUID

For steady state thermal conductivity measurements, time is not a factor in the analysis by definition. The following simple relationship applies:

$$q = \lambda \Delta T / \Delta x \qquad (\ 6.1\ )$$

For various geometries, as has been discussed in Chapter II, the above equation is modified so that thermal conductivity can be calculated directly from heat flow across a fluid, the temperatures at the interfaces, and dimensions of the equipment. As discussed in Chapter II, the problems involved with steady state measurements can be severe.

Transient thermal conductivity measurements are not allowed to reach steady state. Often, as in this work, they are specifically designed for; simplicity of construction and operation, rapid results, and elimination of convection. Unfortunately, the equation describing transient conduction includes thermal diffusivity as a factor. Equation AI.35, written here as equation 6.2,

$$T = qr_0/2\lambda \ \{\ln(4\alpha t/C^{*}r_0^{2}) + (r_0^{2}/4\alpha t) + (r_0^{2}/2\alpha t)/(\ln(4\alpha t/C^{*}r_0^{2})) + (2r_0^{2}/4\alpha t) * (\ln r_0/r)) + \ldots\} \qquad (6.2)$$

describes the temperature distribution in the fluid around a hot-wire as a function of: heat input, filament radius, liquid thermal conductivity, liquid thermal diffusivity, and time. Terms of third and higher order have been neglected. For representative liquids, the ratio of the second, third, and fourth terms of equation 6.2 to the first term is given in Figure 2 for water at 150 C and pentane at 100 C. The thermal diffusivities of these two examples represent a high value and a low value, and are listed in Appendix F. Most organic or aqueous organic liquids have thermal diffusivity values between these two. As shown in Figure 2, the ratio of each individual second order term in equation 6.2 to the first term is small, and becomes smaller with time. Figure 3 shows the ratio of the sum of the second order terms with respect to the first. The contribution of the second order terms relative to the first in equation 6.2 is less than 0.1% at 0.02 second, and quickly decreases to less than 0.005% at 0.5 second. The same behavior would be expected for most organic and aqueous organic liquids due to similar thermal diffusivity values. Removing these second order terms from equation 6.2 gives equation 6.3.

$$T = qr_0/2\lambda\{\ln\ (4\alpha t/C^{*}r_0^{2})\} \qquad (6.3)$$

The thermal diffusivity of a liquid well below its

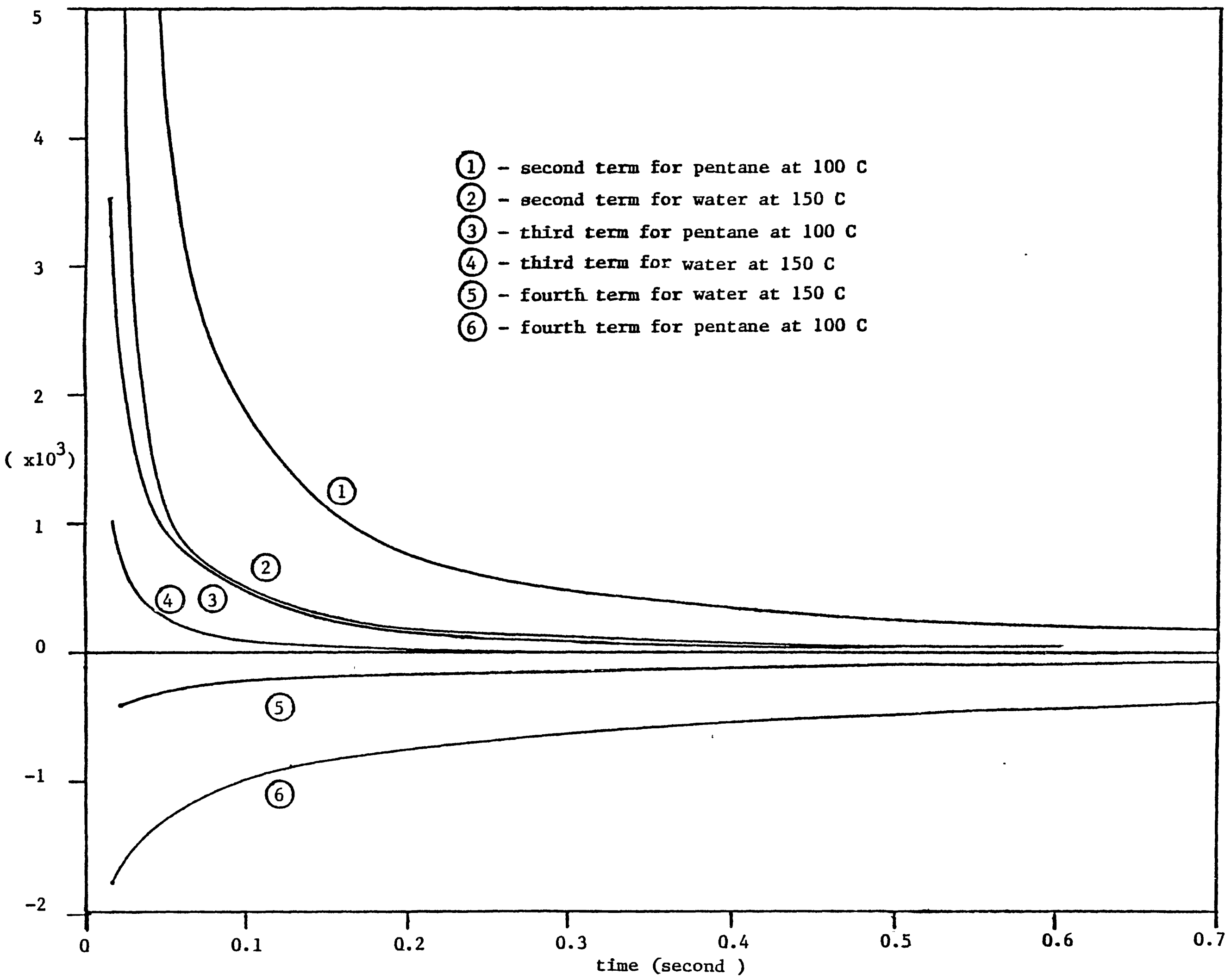

Figure 2. Ratio of Second, Third and Fourth Terms of Equation 6.2 to the First Term

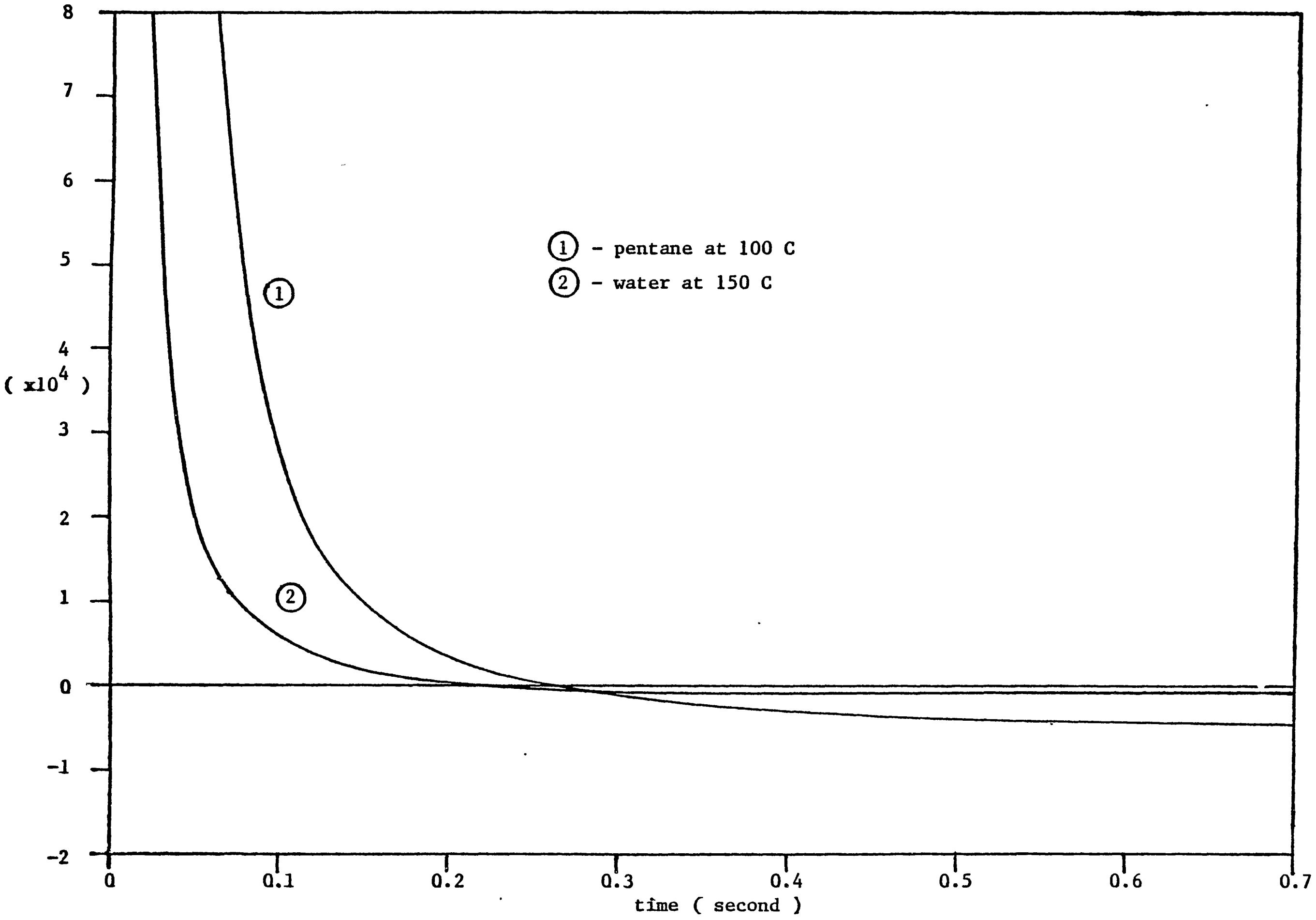

Figure 3. Ratio of the Sum of the Second, Third and Fourth Terms of Equation 6.2 to the First Term

critical temperature does not change greatly with temperature. One could be tempted to separate the logarithmic term into time dependent and time-independent terms, as Lee et al (41), Horrocks and McLaughlin (30), and Mallan et al (48) did;

$$T = qr_0/2\lambda \{\ln (4\alpha/C^* r_0^2) + \ln (t)\} \qquad (6.4)$$

The value of the time independent term does not change much over the course of the measurement, so the above authors chose to write;

$$T = qr_0/2\lambda \{ \ln(t)\} \qquad (6.5)$$

Actually, the measurement begins at a time of zero, which is an initial equilibrium condition given in Appendix A as equation AI.5.

$$\text{at } t = 0, \ T(r,t) = 0 \qquad (6.6)$$

The logarithm of zero is negative infinity and equation 6.5 is undefined at zero time. The thermal diffusivity term cannot be discarded without further analysis.

As derived in Appendix A, and shown in equations AI.50 and AI.51, the thermal conductivity measured by a relative transient method, such as used in this work, depends upon the slope of the ratio of the first term of equation 6.2 for a test liquid to that of the calibrant. Water was the calibrant in this work. This ratio, defined as F_1 , is shown in equation 6.7.

$$F_1 = \{ \ln(4\alpha_1 t/C^* r_o^2)/\ln (4\alpha_w t/C^* r_o^2) \} \qquad (6.7)$$

The behavior of equation 6.7 for several liquids is shown in Figure 4, with water at 20 C serving as the reference. Several liquids at various temperatures represent fluids of various thermal diffusivities. The thermal diffusivity values of these liquids are found in Appendix F. The greater the difference between the thermal diffusivity of the test liquid and the calibrant, the greater the difference in the initial slopes.

The slope, or the first derivative with respect to time of equation 6.7, is:

$$F_1' = [\ln(4\alpha_w t/C^* r_o^2) - \ln(4\alpha_1 t/C^* r_o^2)]/ \\ t(\ln(4\alpha_w t/C^* r_o^2))^2 \qquad (6.8)$$

The behavior of equation 6.8 for several liquids from Figure 4 is shown in Figure 5. The value of the initial slope for the liquids shown with respect to water is not negligible at times less than 0.1 second, as assumed by Lee et al (41), Horrocks and McLaughlin (30), and Mallan et al (48). Therefore, measurements of thermal conductivity using the relative transient method can include the effect of thermal diffusivity if the measurements are made within the first two tenths of a second and the thermal diffusivities of the test fluid and calibrant are greatly different.

The values of thermal diffusivity for hydrocarbons and

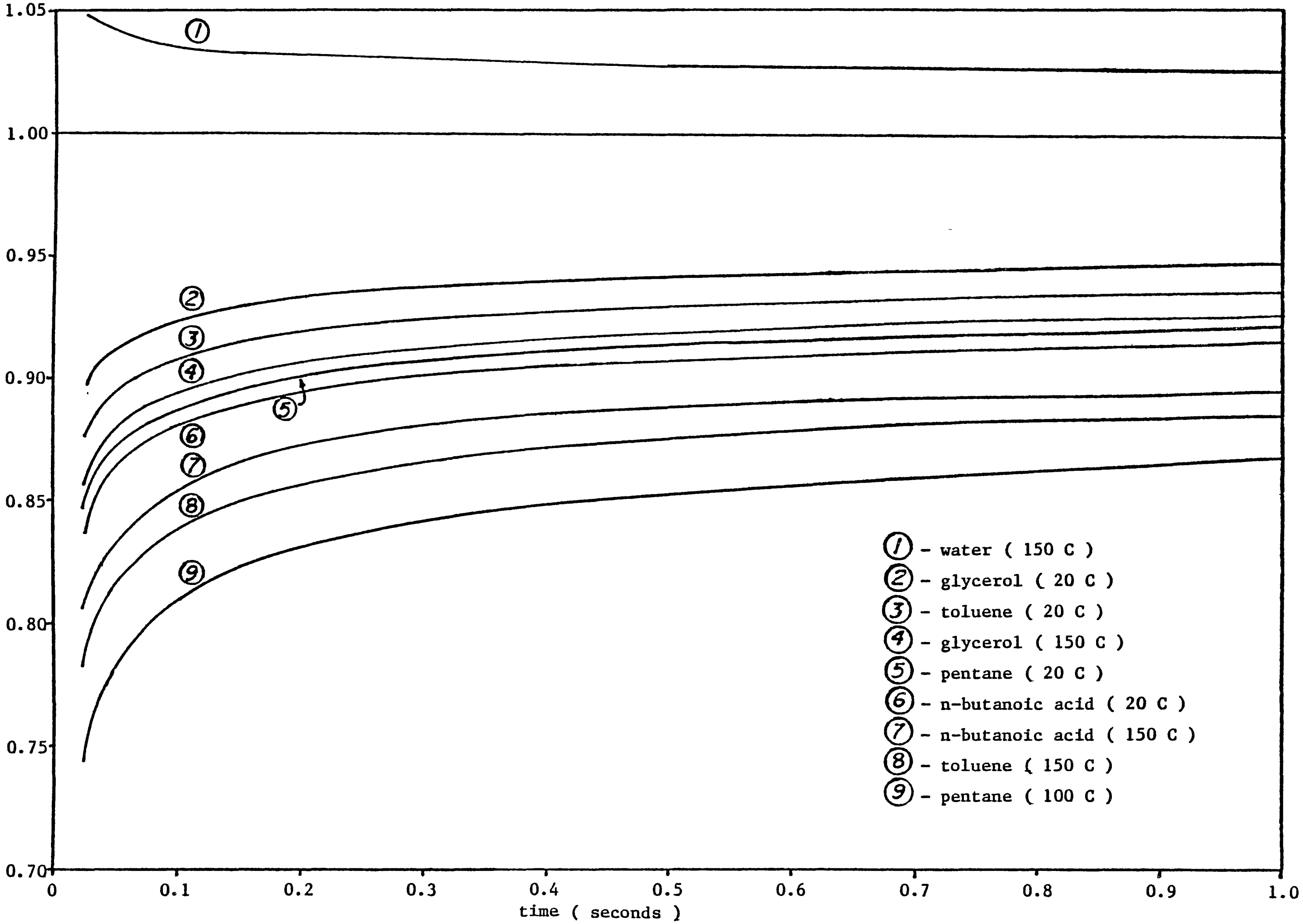

Figure 4. Behavior of Equation 6.7 for Several Liquids

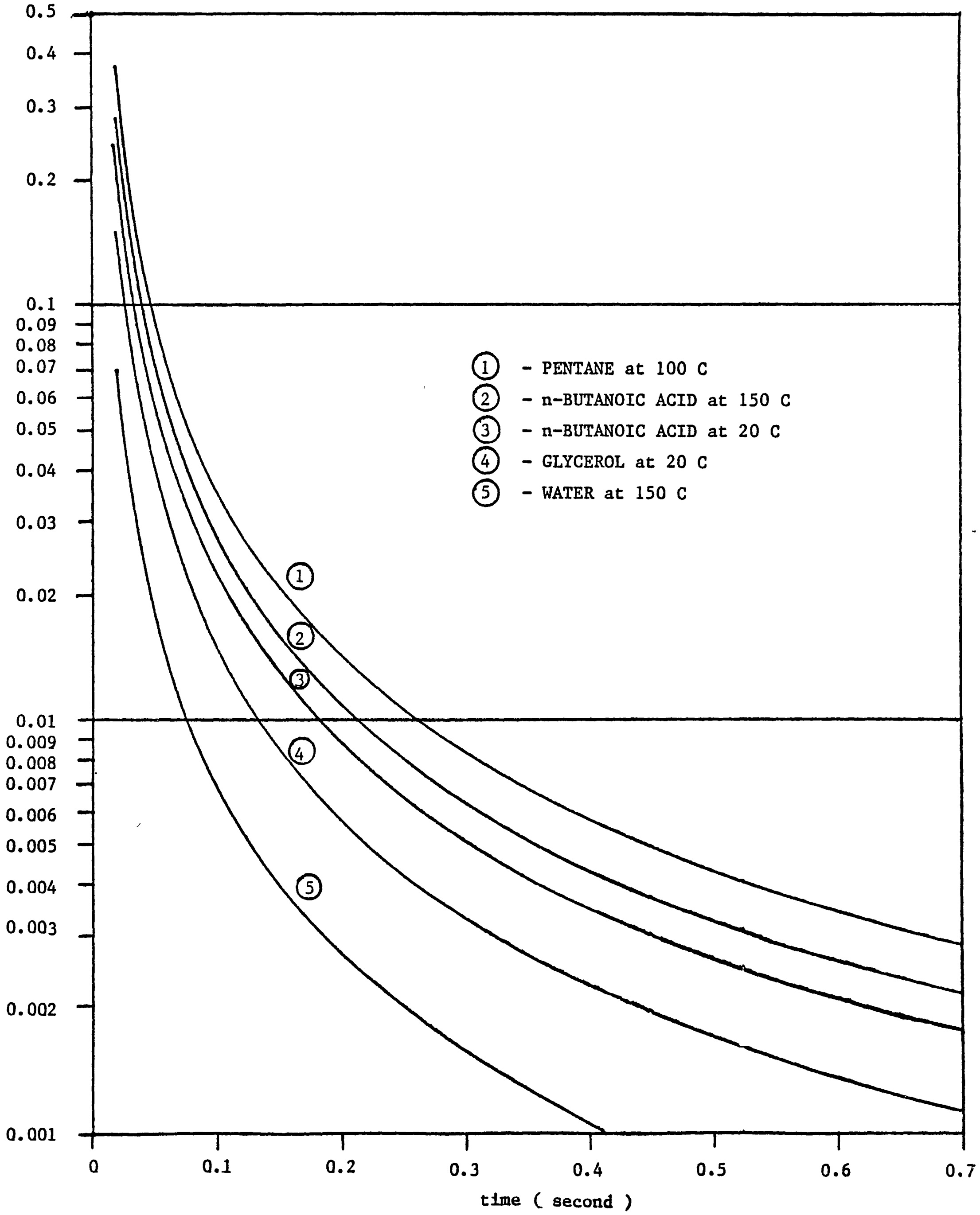

Figure 5. Behavior of Equation 6.8 for Several Liquids

many pure organic liquids are similar. The above-mentioned authors measured principally the thermal conductivity of hydrocarbons and similar fluids. The effect of thermal diffusivity on their measurements was negligible, even though their measurements were extrapolated to zero time, since the fluids which they measured had nearly the same thermal diffusivity as their calibrants. In this work, the thermal diffusivity of the calibrant and measured fluids were very different in some cases, and the effect of thermal diffusivity early in the measurement was significant. Although the value of the slope for the liquids shown in Figure 5 is significant at times less than 0.1 second, at times greater than 0.4 second, the value of the slope becomes very small. Since after 0.4 second the slope became very small, and changed little with time, irrespective of the fluid, all measurements in this work were taken 0.5 second after the step change in voltage was applied to the system which initiated the experiment. The choice of 0.5 second was made for taking the measurement from the X-Y recorder since convection never appeared before 0.8 second.

Before the effect of the thermal diffusivity on the measurement was discovered, measurements of toluene and glycerol extrapolated to zero time, using water as reference fluid, were consistently 20 and 10 % high, respectively, with respect to literature values. Measurements taken at 0.5 second gave results within experimental error of literature values. These results are shown in Figures 6 and 7 for

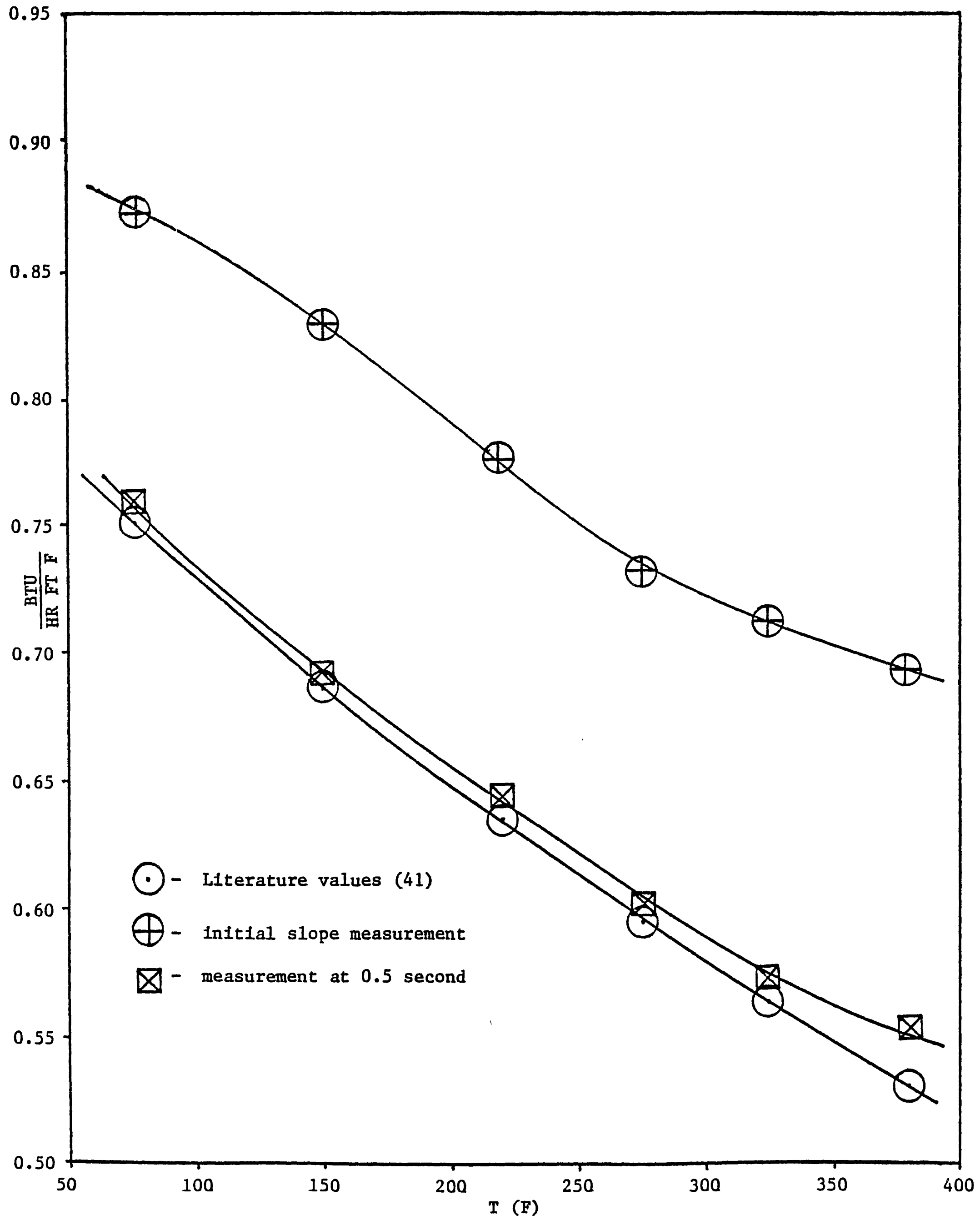

Figure 6. Effect of Time of Measurement on Results for Toluene

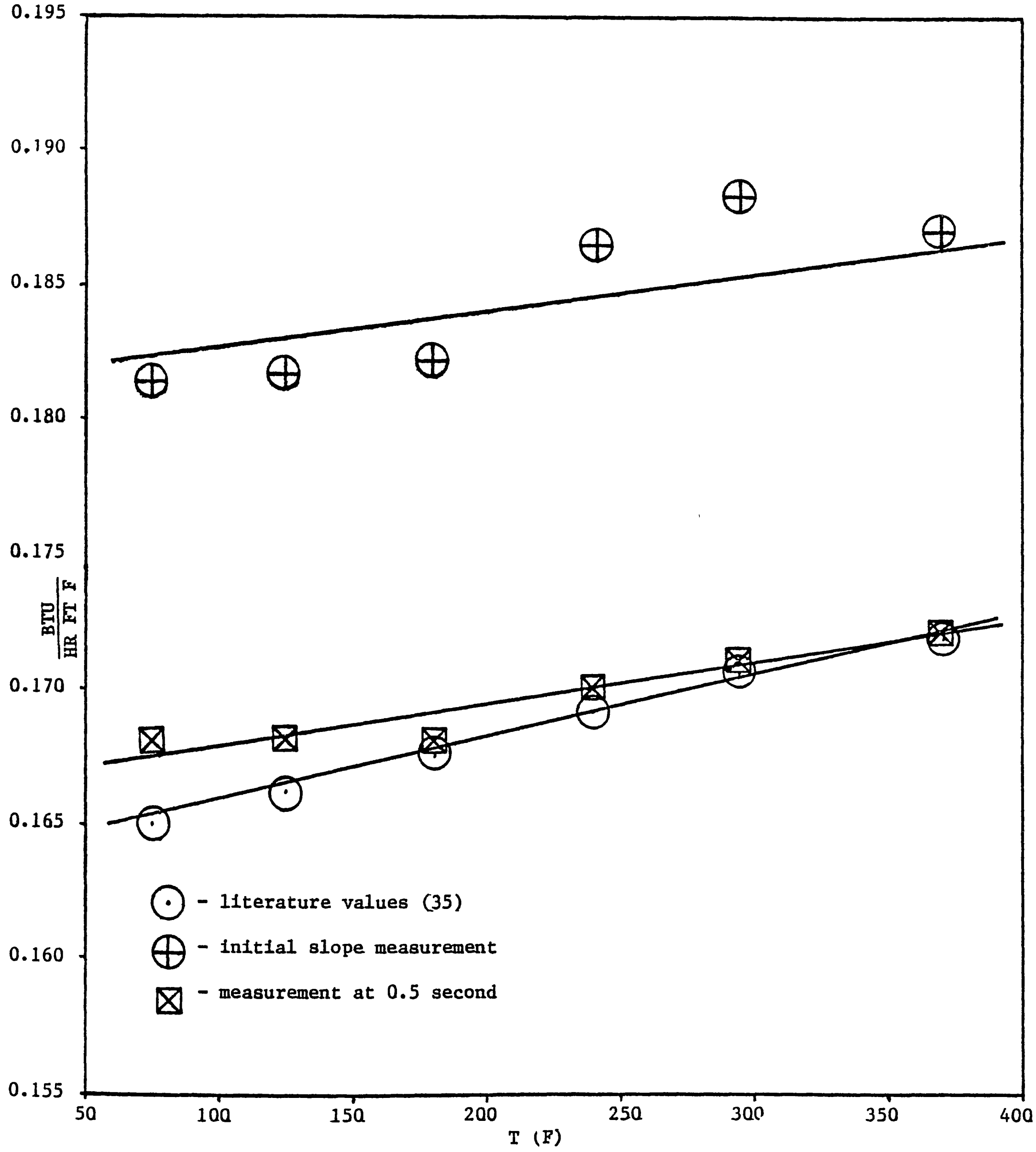

Figure 7. Effect of Time of Measurement on Results for Glycerol

toluene and glycerol, respectively.

For relative steady state measurements the thermal diffusivity does not enter into the measurement. Any fluid of known thermal conductivity can be used for calibration. Toluene, water, and glycerol are the liquids most often used for calibration. For relative transient measurements, the thermal diffusivity can affect the measurement, so the calibration fluid should be chosen carefully. As shown in Figures 4 and 5, the change in slope between 20 C and 150 C is greater for toluene than for water. Therefore, water is a better calibration fluid for a wide temperature range than toluene. Glycerol was not chosen since it is hygroscopic and has not been measured as extensively as water or toluene.

Since the liquids in this work were often aqueous solutions, with thermal diffusivities adjusted toward water and away from toluene, water was again a better choice as a calibration liquid.

The thermal conductivity of water is given in Table I. All three sources reported that their measurements used an absolute method. The agreement between the data is exceptional. The maximum deviation is less than 1.1 %, and the average of the average percent deviation of the second and third data set is 0.37%. The first set of data was used in this work for calibrating the measurement cell.

TABLE I

THERMAL CONDUCTIVITY OF WATER

T (F)	TC (35)	TC (75)	%	TC (5)	%
60	0.3445	0.3409	-1.05	------	-----
80	0.3541	0.3516	-0.71	0.3506	-0.99
100	0.3628	0.3612	-0.44	0.3604	-0.66
120	0.3705	0.3696	-0.24	0.3690	-0.41
140	0.3771	0.3769	-0.05	0.3765	-0.16
160	0.3829	0.3831	+0.05	0.3827	-0.05
180	0.3876	0.3881	+0.12	0.3879	+0.08
200	0.3915	0.3920	+0.13	0.3919	+0.10
220	0.3944	0.3948	+0.10	0.3949	+0.13
240	0.3964	0.3964	0.00	0.3968	+0.10
260	0.3976	0.3969	-0.18	0.3978	+0.05
280	0.3978	0.3962	-0.40	0.3978	0.00
300	0.3973	0.3950	-0.58	0.3969	-0.10
320	0.3958	0.3932	-0.66	0.3950	-0.20
340	0.3936	0.3907	-0.74	0.3923	-0.33
360	0.3906	0.3875	-0.79	0.3887	-0.49
380	0.3867	0.3835	-0.83	0.3844	-0.60
400	0.3821	0.3788	-0.86	0.3793	-0.73

THE EQUATIONS GIVEN IN THE STATED REFERENCES USED TO GENERATE THE ABOVE DATA ARE:

Jameison et al (BETWEEN 32 AND 400 F)

$$TC = 0.30921 + 6.6707 * 10^{-4} *T(F) - 1.3455 * 10^{-6} *T^{2} (F) + 3.3391 * 10^{-9} *T^{3} (F)$$

Thermophysical Properties of Matter, vol. 3
(BETWEEN 32 AND 284 F)

$$TC = -0.336382 + 3.67549 * 10^{-3} *T(K) - 4.60590 * 10^{-6} *T^{2} (K)$$

(BETWEEN 284 AND 644 F)

$$TC = -0.082210 + 2.38684 * 10^{-3} *T(K) - 2.97657 * 10^{-6} *T^{2} (K)$$

TABLE I CONTINUED

Amirkhanov et al (BETWEEN 77 AND 662 F)

$TC = 0.321776 + 1.22232 * 10^{-3} *T(C) - 5.42 * 10^{-6} *T^{2} (C)$
$+ 4 * 10^{-9} *T^{3} (C)$

** NOTE: ALL THERMAL CONDUCTIVITY DATA IS REPORTED IN BTU/HR FT F

CHAPTER VII

MODIFICATION OF THE WHEATSTONE BRIDGES

The X-Y recorder receives an amplified voltage signal from the reference and test cell bridges. The measurement in this work involves a comparison of these signals. The signal sent to the differential amplifiers by the bridges is a voltage difference caused by a resistance difference between the decade resistor and the filament when the filament heats. The resistance change of both filaments over the course of the measurement is 0.018 ohm each. The smallest division on the decade resistors is 0.01 ohm, which is relatively large in comparison to the total change. By balancing each filament to the closest division of its decade resistor, a balance to the closest 0.005 ohm can be achieved. A total imbalance of 0.005 ohm in this apparatus changed the X-Y recorder slope by approximately 2 to 3 percent. Instead of measuring and compensating for the bridge imbalance errors, a way was found to eliminate them.

Decade resistors are generally available with three to five decades of resistance adjustment. Accurate resistance divisions below 0.01 ohm are difficult to manufacture because switch resistances become as large or larger than

0.001 ohm. Generally, the smaller the division of resistance on a decade resistor, the more complex and expensive it becomes.

For the thermal conductivity measurement in this work, only the absolute voltage and resistance values need be known. As shown in Appendix B, the maximum error contributed by the absolute resistance uncertainty is approximately 0.1%. However, minute resistance imbalances in a bridge circuit alter the slope of the line drawn by the X-Y recorder. An adjustable small resistor, in series with each decade resistor, with a range of approximately 0.02 ohm, was needed to eliminate the bridge imbalance error while not appreciably affecting the absolute resistance measurement.

At first, a slide wire resistor using the same tantalum used for making the support wire was inserted in series with each decade resistor. These units were cumbersome to use and did not give a steady balance on the null detector due to the contact resistance on the wire. Since low resistance adjustable resistors in series did not work, high resistance adjustable resistors were tried. As indicated in Figure 8, two series resistors, one a fixed 33 kilo-ohm resistor and the other a variable 0 to 2.5 mega-ohm resistor, were installed parallel to each decade resistor. The dual parallel resistors allowed each decade resistor to be balanced to the maximum sensitivity of the null meter which, for this apparatus, was approximately 10 micro-ohms, or 0.1

LEGEND FOR FIGURE 8

TC - THERMAL CONDUCTIVITY TEST CELL
RC - THERMAL CONDUCTIVITY REFERENCE CELL
DA1 - TEST CELL DIFFERENTIAL AMPLIFIER
DA2 - REFERENCE CELL DIFFERENTIAL AMPLIFIER
ND - NULL DETECTOR
XY - X-Y RECORDER
S1 - MEASUREMENT SWITCH
P1 - POWER SUPPLY FOR TEST CELL
P2 - POWER SUPPLY FOR REFERENCE CELL
tm - TIME OF SLOPE MEASUREMENT
Θ - ANGLE OF SLOPE
R1 - DECADE RESISTOR TEST CELL
R2 - FIXED RESISTOR (33,000 OHM)
R3 - VARIABLE RESISTOR (0 TO 2.5 MEGA-OHM)
R4 - PRECISION RESISTOR (100.0 OHM)
R5 - PRECISION RESISTOR (100.0 OHM)
R6 - DECADE RESISTOR REFERENCE CELL
R7 - VARIABLE RESISTOR (0 TO 2.5 MEGA-OHM)
R8 - FIXED RESISTOR (33,000 OHM)
R9 - PRECISION RESISTOR (100.0 OHM)
R10 - PRECISION RESISTOR (100.0 OHM)

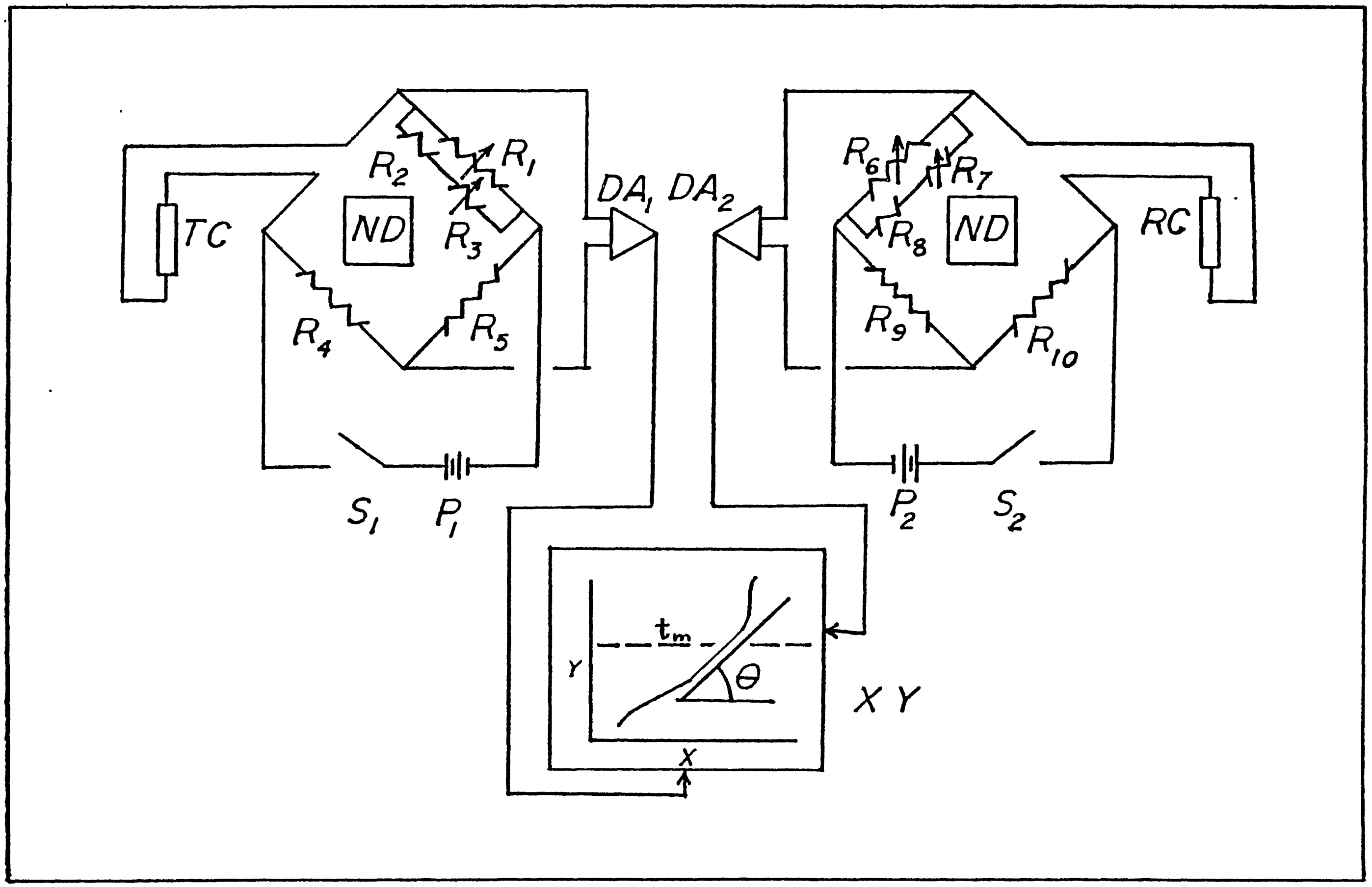

Figure 8. Apparatus Schemeatic

percent of the smallest division on the unmodified decade resistor. Because the dual parallel resistor resistance was always larger than the filament resistance by a factor of 1000, no more than 0.1 percent of the current was allowed to pass through the dual resistor. A 0.1 percent shunt of the current would cause an equal error in the measurement. Therefore, the 2 to 3 percent error caused by bridge imbalance was traded for a maximum 0.1 percent error through use of the dual parallel resistors in each Wheatstone bridge circuit.

CHAPTER VIII

TEMPERATURE LIMITATIONS

Miller (51) indicates that a tantalum oxide coating can be useful as an electrolytic capacitor to 200 C. The oxidized filament in this work is essentially an electrolytic capacitor, except the sulfuric or silicic acid electrolytes used in commercial capacitors are replaced by the solution measured. Sisco and Epremian (70) show that as the temperature of the capacitor rises, current leakage increases dramatically. For example, for every 60 C increase in temperature, the current leakage increases approximately 1000 percent. Therefore, at 300 F, the current leakage in the filament should be nearly 100 times that at 80 F.

The resistance of the oxide coating changed during the measurement. At room temperature, the oxide coating consistently gave an initial resistance of 3 to 5 mega-ohms. After heating the filament to about 300 F, the oxide coating exhibited a nominal resistance of 50 to 100 kilo-ohms. At 400 F, the resistance dropped to approximately 1000 ohms, or about 0.05 percent of the original resistance. As the resistance change occurred without respect to the solution, and the color of the oxide coating did not change, the decrease in resistance was probably due to micro-cracks in the coating caused by the metal filament and support wire expanding more than the oxide coating. Re-oxidation was complete in less than 10 minutes, proving that the amount of exposed metal surface was small.

A normal thermal conductivity measurement, as will be discussed in Chapter IX, appears as a curve on the X-Y recorder. The curve should be nearly linear at first, with a gently increasing slope, becoming fully linear near the time of measurement. Between 300 and 400 F, the X-Y recorder pen would momentarily deflect in the negative horizontal (X) direction and positive vertical (Y) direction. This "bump" invalidated the measurement. The temperature at which the bump occurred was not reproducible, but almost always occurred between 325 and 375 F. The bump was probably due to a decrease in resistance of the oxide at elevated temperature. With increasing temperature, the tantalum wire would expand more than the oxide, cracking the uniform oxide layer and exposing some of the tantalum to liquid. The oxide, if cracked, would have a lower apparent resistance. Additionally, as the oxide layer temperature increases, its resistance decreases even if not cracked (51). Attempts were made to increase the useful temperature of the filament by performing the anodic oxidation in the sulfuric acid solution at 120 to 150 F. No improvement in the temperature range was observed.

CHAPTER IX

MEASUREMENT OF THERMAL CONDUCTIVITY

A relative hot-wire apparatus was used in this work to measure thermal conductivity of aqueous and pure liquid organic acids. The basic apparatus is thoroughly explained by Nangia and Chenoweth (53). The equipment and materials descriptions and specifications are given in Table II. Each filament wire was made one arm of a Wheatstone bridge, as shown in Figure 8. Before measurement, the resistance of the filament was measured and balanced with the null detector using the decade resistor and variable potentiometer in each bridge. Known step voltages were then impressed across both wires simultaneously. The filaments, heated by the electrical current, emitted heat to the liquid surrounding the filament. The amount of heat removed by a fluid is a function of its thermal conductivity. Since the fluid thermal conductivity is less than that of the filament, the filament temperature increases, causing the filament resistance to increase. The temperature change in each wire was a function of the electrical heat supplied to the filament and the thermal conductivity of the fluid.

The change in resistance of each filament was measured as a change in voltage in each Wheatstone bridge. Each small voltage change was amplified by the differential amplifiers and X-Y recorder by a known and equal amount. The X-Y recorder recorded: the amplified voltage change with time, the reference filament change on the vertical axis, and the test filament change on the horizontal axis. When the rate of resistance change for each filament was the same, the X-Y recorder drew a straight line at a 45 degree angle.

The derivation of the basic equation for heat transfer in a filament is given in Appendix A. The result was used in the derivation of the equation relating the heat transfer in the filament to the thermal conductivity of the liquid around the filament. The final form of the equation is:

$$\lambda_t = \{C_0(T)/\tan\Theta\}\ [(V_t/V_r)^3\ (R_r/R_t)^2] \qquad (9.1)$$

Calibration

The measurement cell was calibrated before fluids of unknown thermal conductivity were measured. The calibration fluid used in this work was distilled water. Many good references exist for the thermal conductivity of water. The one chosen for this work was the Engineering Science Data Unit (ESDU) data published in 1967 (35). More recent work (5,75) agrees quite closely with the ESDU data. Data from all three sources (5,35,75) are shown in Table I and agree within 1.1% at all temperatures, but usually within 0.5%. The deviation of the second and third data sets from the ESDU data is also given in Table I. The average value of the average absolute percent deviation for the two data sets is 0.37%. This is well within the claimed absolute accuracy of 2% for the data.

Preparing the Sample

The glass tube, shown in Figure 1, was removed from the pressure bomb and filled to a point such that the top of the filament was below the liquid surface when the cell was assembled. The filled tube was placed in the pressure bomb, followed by the o-ring pressure seal. The measurement cell top, which held the measurement wire, was carefully brought down into the liquid. The teflon coated clamps, shown in Figure 1, prevent the oxidized wire from scraping against the wall of the glass tube. Once the measurement cell was assembled, it was connected to the electronic system using the low resistance gold-plated multi-pin connectors. The assembled cell was then immersed in the bath and allowed to reach thermal equilibrium. The duplicate reference cell is filled with silicone oil and maintained at 32 F in an ice-water bath. The reference cell was not opened after initial preparation.

Measurement of X-Y Recorder Output

First, the resistance of each filament was determined to 0.01 ohm by balancing it against its respective decade resistor. Using the null meter at high sensitivity, such that a change of 10 micro-ohm could be detected, the potentiometer, in parallel with the decade resistor, was adjusted to balance the filament against the decade resistor-potentiometer arm in the Wheatstone bridge. The electrical potential across the reference cell was maintained at 2.000 volts. As the reference cell was maintained in a water and ice bath, its resistance was nearly constant. The absolute resistance of the test wire changed with temperature. Unchanging resistance in the test wire indicated the test cell was in thermal equilibrium with the bath. The temperature of the bath was measured with the millivolt potentiometer when the test cell had reached thermal equilibrium. The test and reference cell voltages and resistances were recorded before measurement. A switch was used to connect the power supply to both filaments at the same time, which started the measurement. The X-Y recorder recorded the relative change in resistance of each wire. At exactly 0.5 seconds, the slope of the line drawn by the X-Y recorder was measured. If the slope was not 45.00 degrees, indicating unequal temperature changes for the filaments, the voltage of the test cell was adjusted and the measurement was repeated after the test and reference cells returned to thermal equilibrium.

Calculation of Thermal Conductivity

From the voltage and resistance measurements taken during the slope measurements, and using equation 9.1, the thermal conductivity of a liquid can be measured. Six to eight data points were taken in eight to twelve hours, depending upon the stability of the bath temperature and rate at which the bath was heated. The present apparatus is capable of measuring fluid thermal conductivities from 32 to 300 F and atmospheric pressure to 1000 psig.

Convection

At times between 0.8 to 6.0 seconds, depending upon the test fluid viscosity, thermal diffusivity, and temperature, convection appeared in the measurement as a definite departure from the linear response on the X-Y recorder.

The resistance change of the test fluid was recorded on the X axis, and that of the reference fluid was recorded on the Y axis, as indicated in Figure 8. During conduction, the relative change in resistance of the filaments was linear. Convection in a fluid around a filament reduces the temperature rise rate of the wire as more heat enters the fluid. The reference fluid was cool and highly viscous relative to the measurement fluid. Thus, convection appeared in the test fluid first, and was seen as an abrupt upward curve. The curve slopes upward because the test filament, influenced by convection in the surrounding liquid, did not heat as fast as the reference fluid, which was affected only by conduction.

Re-oxidation

After measurements were taken above 250 F, the test filament was re-oxidized. Re-oxidation was accomplished by re-connecting the test wire anodically in an electrolytic cell and exposing it to a curent density of 1 milliamp per square centimeter as described in Chapter IX. The need for re-oxidation is explained in Chapter VIII. The time required for re-oxidation was less than 10 minutes.

Proof of Coating

The filament coating resistance could not be measured with the filament in the cell. The integrity of the coating was proven otherwise. After a 45 degree slope was attained for a measurement by adjusting the test cell voltage, the reference and test cell voltages were changed such that their ratio remained the same. If the slope did not change more than 0.5%, the reproducibility of data in this work, the coating was intact. If the slope changed more than 0.5%, the coating was assumed cracked or conductive, and the measurement discarded.

A bare and an oxidized wire were tested separately in distilled water at 75 F. Table III indicates the oxide coated filament gave a consistent value for the voltage and resistance term of equation 9.1 for each of the three voltage pairs. The bare wire gave different values at each of the voltage settings, as some of the electrical energy from the bare wire acted directly on the water.

TABLE II

INSTRUMENTS, EQUIPMENT, AND MATERIALS

---

1. Constant Temperature Bath -
    Neslab Instruments, Inc., model TEV70/HIGH
    Range: 0 to 250 C
    Capacity: 18.5 gallons
    Duty Available: one 800 and one 1250 watt heater

2. Constant Temperature Bath Fluid -
    General Electric, Inc., liquid dimethyl polysiloxane
    product type SF-96, viscosity grade 200 cs at 25 C
    Recommended Useful Temperature Range: -40 to 500 F
    Flash Point: above 600 F

3. Millivolt Potentiometer -
    Leeds and Northrup, Inc., model 8686
    Range: -10.1 mV to +100.1 mV
    Limit of Error: ±0.05%
    Resolution: 0.005 millivolt

4. Bath Temperature Controller -
    Fisher Scientific Co., model 15-177-50
    Temperature Range: 0 to 250 C
    Sensitivity: 10% change in output for 0.01 C change
    Temperature Control: 0.01 C
    Temperature Setting Reproducability: ±0.02 C
    Total Power Output: 1500 watts

5. Differential Amplifiers -
    Hewlett/Packard, model no. 8875A
    Gain Settings: OFF,10,20,50,100,200,500,1000
    Gain Accuracy: ±0.1%
    Gain Stability: ±0.01% for 30 days
    Non-Linearity: less than 0.01%
    Settling Time: 99.9% within 0.1 millisecond

6. Direct Current Power Supply -
    Hewlett/Packard, model no. 6213A
    Output: 0 to 10 VDC
    Noise: less than 200 microvolts
    Stability: less than 0.1% drift for eight hours

TABLE II CONTINUED

7. Voltmeters -
   Digitec Co., model 2870 , series HT
   Resolution: 1 millivolt
   Accuracy: ±2 millivolt
   Response Time: 99.99% within 0.85 seconds upon 20 volt step change

8. Null Detector -
   Leeds and Northrup, Inc., model 2437-1
   Sensitivity: 0.5 microvolt
   Noise: less than 0.5 microvolt
   Stability: less than 1.0 microvolt change per hour

9. Decade Resistors -
   General Radio Co., model 1433-U
   Range: 0.00 to 111.1 ohms
   Step Changes: 0.01, 0.1, 1, 10 ohms
   Accuracy: ±(0.02% + 2 milliohms)
   Switch Resistances: less than 0.0005 ohm
   Maximum Coefficient of Resistance: ±20 ppm/ C

10. X-Y Recorder -
    Bausch & Lomb, model 2000 Omnigraphic, type 3
    Acceleration: greater than 1500 inches per second squared
    Overshoot: less than 1% on full scale steps
    Accuracy: ±0.2% of full scale
    Linearity: ±0.1% of full scale
    Repeatability: ±0.1% full scale
    Resetability: ±0.05% full scale
    Adjustability: zero over 110% of scale
    Settings: decades of 1 to 10,000 mV per inch

11. Adjustable Pressure Regulator -
    Grove Co., model 15LH
    Range: 0 to 1000 psig

12. Pressure Gauge -
    US Gauge Co., model - test gauge
    Range: 0 to 1000 psig
    Accuracy: 0.2% full scale
    Smallest Division: 5 psi

13. Tantalum -
    A.D. Mackay Co., 99.95% pure metal
    support wire - 0.035 inch diameter
    filament - 0.001 inch diameter

TABLE II CONTINUED

14. Formic Acid -
    Fisher Scientific Co., grade - certified
    89.0 wt% formic acid by analysis
    0.2 wt% acetic acid

15. Acetic Acid -
    Fisher Scientific Co., grade - reagent, glacial
    99.70 wt% minimum acetic acid
    0.01 wt% acetic anhydride

16. Propionic Acid -
    Fisher Scientific Co., grade - reagent
    99.75 wt% minimum propionic acid
    0.02 wt% water by analysis

17. n-Butanoic (Butyric) Acid -
    Fisher Scientific Co., grade - reagent
    99.75 wt% minimum butyric acid
    0.02 wt% water by analysis

TABLE III

VOLTAGE AND RESISTANCE TERMS FOR INSULATED AND UNINSULATED FILAMENT AT 75 F IN WATER

Vt	Vr	Rt	Rr	(Vt/Vr)*(Rr/Rt)	STANDARD DEVIATION
INSULATED WIRE -					
2.020	1.500	24.65	28.45	3.253	0.012
4.040	3.003	24.65	28.45	3.243	(0.37 %
10.000	7.415	24.65	28.45	3.267	of avg.)
UNINSULATED WIRE -					
2.214	1.500	29.69	28.46	2.955	0.408
5.496	3.500	29.69	28.46	3.558	(11.9 %
12.765	8.000	29.69	28.46	3.733	of avg.)

CHAPTER X

RADIATION

According to Menashe et al (50), for hot-wire devices, the radiant contribution to the thermal conductivity of toluene can be as much as 3%. They make similar calculations for n-heptane, n-octane, and n-undecane. These compounds are weak absorbers of infrared radiation. For materials which absorb infrared radiation more strongly (water, alcohols, organic acids, and chlorinated organic compounds) the radiation contribution to the thermal conductivity will be much greater.

Gurenkova (26) shows through interferometry that, in a flat plate cell at steady state, the apparent radiation contribution to the heat transfer is a function of the fluid layer thickness for several hydrocarbons, but is not for water, ethanol, or propanol due to their strong absorption of infrared radiation. This evidence contradicts the theory of Menashe et al (49). Many authors (4,5,19,22,26,27,29, 33,44,46,49,52,54,62,75,78) recognize the potential problem of the radiant component of heat transfer as a complication in their measurements, but conclude that for fluids which absorb infrared radiation strongly, such as water, alcohols, and organic compounds containing a carbonyl or carboxy functionality, the effect of radiation is negligible. For strong absorbers, infrared radiation is quickly converted to heat before it can be re-emmited. The treatment of the radiation component by Menashe et al (50) was purely mathematical and only applicable to devices which extrapolate measurements to zero time.

For the apparatus described in this work, the resistance rise for the wires over the course of the measurement time of 0.50 second was 0.0180 ohms. The temperature coefficient of the filament was found to be 0.042 ohms/F to within 0.3%. The temperature rise during the course of the experiment was, therefore, 0.42 F, or 0.23 K. Horrocks (30), Healy (29), and Kirk-Othmer (37) give the maximum heat transfer contribution of the radiation component for a hot wire as:

$$Q_{rad} = 2\pi r\sigma\ (T_1^4 - T_w^4) \qquad (10.1)$$

The Stefan-Boltzmann constant, σ, is $5.67 * 10^{-8}$ W/m^2K^4. The radiative contribution is a function of temperature. The range of this work is from 70 to 350 F, or approximately from 300 to 450 K. As calculated in Appendix C, at 300 K and 450 K the radiant heat output would be 388 and 155 microwatts per meter, respectively. According to equations AI.46 and AI.47, shown below as equations 10.2 and 10.3, respectively:

$$\Delta T_y = q_y/\lambda_y \qquad (10.2)$$

$$\Delta T_x = q_x/\lambda_x \qquad (10.3)$$

For equal constant heat input to the filament, the temperature change of the fluid surrounding the filament is inversely proportional to the fluid thermal conductivity. The equation for electrical heating is:

$$Q_{el} = (V^2/R)\Delta t \qquad (10.4)$$

The electrical heat output from the filament for n-butanoic acid is 620 and 640 milliwatts per meter, at 75 and 308 F, respectively, as shown in Appendix C. The maximum radiant contribution at 70 and 308 F is 0.018 and 0.052 percent of the electrical resistance heating, respectively. For water, the maxima are 0.0070 and 0.021 percent at 73 and 360 F, respectively, as is also shown in Appendix C.

The above analysis is only appropriate for totally transparent fluids. The organic acids and water used in this work are nearly opaque to infrared radiation in the thermal range of 6 to 10 microns wavelength (59), which corresponds to a temperature range of 20 to 200 C. The calculated maximum radiation contributions, although small, are still too large for these strong infrared absorbers. Kirk-Othmer (37) gives the total emissivity of water as 0.96. For water, the calculated maximum radiation contribution should be reduced by the emissivity factor, or to 4% of the calculated maximum to obtain the true maximum. For alcohols and organic acids, the total emissivity should be nearly as large, probably between 0.85 and 0.95. The maximum radiant contribution for n-butanoic and the other acids would be reduced to at most 15% of the maximum calculated for transparent liquids. The resulting true maximum radiant contribution of 0.003%, as shown in Appendix C, is negligible.

The radiant contributions to the thermal conductivity measurements in this work were small due to the short heating times and the minute temperature changes employed. Indeed, the effect of radiation in a transparent fluid, shown above to be at most 0.052%, could be neglected using this instrument.

CHAPTER XI

MEASUREMENT ERROR SOURCES

The hot-wire method for determining thermal conductivity is approximated by an infinite line source, as is explained by Carslaw and Jaeger (15). Healy et al (29) present a complete theory for the finite hot-wire, and resolve several potential error sources analytically. Raal (62), Le Niendre (44), Irving (33), Nagasaka (52), and Geller (19) discuss other equipment oriented potential error sources.

Perfectly Cylindrical Filament

According to Carslaw and Jaeger (15) and Healy et al (29), a perfectly cylindrical filament is not necessary for accurate thermal conductivity measurements when $4\alpha t/r^2$ is greater than 10. As shown by calculation in Appendix D, $4\alpha t/r^2$ ranges from 820 to 1790 for for a measurement time of 0.5 second for the fluids measured in this work. The filament in this work gave accurate measurements, even though it was not proven perfectly cylindrical.

Finite Properties

The hot-wire has finite dimensions and physical properties. These are not included in the general derivation of the equation AI.52 for heat transfer from the hot-wire in Appendix A. Healy et al (29) present a lengthy derivation for heat transfer to a fluid from a wire of finite properties. Their analysis shows that the finite heat capacity and thermal conductivity of the wire can be neglected as factors for measuring the thermal conductivity of liquids. The absolute temperature change measured will be shifted slightly versus the logarithm of time in equation AI.36:

$$T = qr_0/[2\lambda \; \{\ln \; (4\alpha t/C^*r_0^2)\}] \qquad (11.1)$$

but the slope of this line, from which the thermal conductivity is determined, will not be affected.

Expanding Temperature Gradient

As the wire heats the fluid, the boundary condition that requires the fluid at infinite distance from the wire to remain at its initial equilibrium temperature may be incorrect. Healy et al (29) show that for transient measurements, the boundary condition is definitely satisfied when the temperature gradient in the liquid does not penetrate far into the liquid.

As calculated in Appendix D, the penetration distance of the temperature gradient into the liquid is on the order of 1.0 mm. As the wire is situated about 5 mm from the glass tube wall in this work, the effect of the expanding temperature gradient on the above boundary condition is negligible.

Variable Fluid Properties

Healy et al (29) analyzed the effect of fluid property changes for steady state experiments, where the temperature change may be several degrees. For fluids far from their critical temperature and pressure, most properties, such as heat capacity, viscosity, and density, do not change enough to alter thermal conductivity measurments. However, they concluded that for liquids in the critical region, where density changes severely with temperature, thermal conductivity measurements would be subject to convection due to variable pressure. The liquids and solutions measured in this work are far below critical, so variability in fluid properties has been neglected.

Non-Constant Heating Rate

The equations for the hot-wire apparatus assume that the heating rate will be constant over the course of the measurement. For cell designs that incorporate two different length filaments with different resistances in

Wheatstone bridge circuits, the relative heating rate will be different. An equation given by Raal et al (62) can be used to calculate the correction to the heat added to each wire;

$$q = q_M [1 + R_s \eta \Delta T] \qquad (11.2)$$

where R_s is the temperature coefficient of the filament, and η is the change in bridge resistance for the measurement divided by the total bridge resistance before the measurement. The resistance change in each bridge in this work during an experiment is small relative to the total resistance of the bridge. The temperature change and resistance temperature coefficient are small, also. As calculated in Appendix D, the change in heating rate is approximately one millionth of one percent for this apparatus. This factor would not be negligible in steady-state experiments which have large temperature differences for wires of small resistance.

Convection

This factor is one of the more important potential errors, as a small amount of convection can transfer a large amount of heat. For parallel surface methods, convection is the most difficult error to detect. Le Niendre et al (44) assert that as long as the product of the Prandtl and Grashof numbers (Rayleigh number) does not exceed 1000, convection will not occur in a fluid. However, this is an assumption. Since the onset of convection was detectable in the measurements for this work, as explained in Chapters VI and IX, this source of error has been eliminated from the data presented here.

Coating on Wire

Nagasaka and Nagashima (52) used a platinum wire coated with a polyester for their transient hot-wire measurements on salt solutions. Their wire coating thickness was approximately 20% of the diameter of their wire, which was 40 microns in diameter. Their measurements were absolute, so they included the heat capacity and thermal conductivity of the coating in their heat conduction equations. They calculated a 0.15% error possible in their measurements due to the insulation for measurements up to 5 seconds. The oxide coating thickness in this work is approximately 1% of the wire diameter. The relationship which shows the effect of the insulation on the thermal conductivity measurement is:

$$\Delta^2 T = (1/t) \ln (r_1/r_0) C_x \qquad (11.3)$$

where;

r_1 = radius of insulated wire

$\Delta^2 T$ correction = correction to the temperature change slope

C_x = time and insulation independent terms

As calculated in Appendix D, the possible error in this work from this factor for a single wire is approximately 0.1%. The reference wire in this work was coated in the same manner as the test wire. Because the resistance change for the test and reference filaments was the same for each measurement, as measured by a 45 degree slope on the X-Y recorder, the error due to thermal resistance of the coating is duplicated in both wires simultaneously, and therefore cancels out.

Support Wire-Filament Junction

Irving and Jameison (33) have determined the potential error contributed to the measurement by the resistance of the support wire and the heat conducted in it during the measurement. Factors that affect this end loss are wire length, filament and support wire diameter, and fluid thermal conductivity. They concluded that, for water, no end loss correction is necessary due to its high thermal conductivity, and that the maximum error should be 3% for their apparatus for liquids of low thermal conductivity. By calibrating their cell, they eliminated the effect of the end loss. As calculated in Appendix D, the maximum junction heating error in this work is only 2% of that incurred by Irving and Jameison (33), or at most 0.06% of the measured value. However, even this small error can be neglected because the test wire was calibrated.

Strain

Wire strain caused by different thermal expansion coefficients of the cell and filament can add error to the measurement. Wires that are fixed at both top and bottom of a cell are subject to strain induced voltages. Since strain is not easy to measure on such a fine filament, many authors eliminate this effect by attaching one end of their filament to a spring (4,33,42,44,52). The spring mechanism is small, delicate, and complex to build. The filament in this work was not subject to strain as it was not attached at the bottom, as is shown in Figure 1. Neither was the filament subject to slackening. After the filament was fixed to the support wire in the thermal conductivity cell top, the linear thermal expansion coefficient of the support wire and filament would be the same, as both were pure tantalum. Damage to the oxide coating due to tantalum thermal expansion is discussed in Chapter VIII.

Inexact Resistance Balancing

The filament resistances in this work were balanced against the known resistance of an accurate decade resistor. The resolution of the decade resistor was 0.01 ohm, while the entire resistance change in either filament was 0.0180 ohm. Generally, the decade resistor alone could not be used to balance the filament. On the equipment used in this work, an imbalance in the resistance of 0.01 ohm changed the slope of the output line by 4 to 6%. The adjustable potentiometer, in parallel with the decade resistor, was used to balance the filament to within 10 micro-ohms, such that no deflection was detected with the null meter at highest sensitivity.

CHAPTER XII

EXPERIMENTAL RESULTS

The thermal conductivity data for pure and aqueous solutions of formic, acetic, propionic, and n-butanoic acids are given in Tables IV, VI, VII, X in Appendix E and shown here in Figures 9, 11, 13 and 15. Thermal conductivity of the pure acids is given in Tables V, VII, IX, and XI in Appendix E and shown here in Figures 10, 12, 14, and 16 for easier comparison of data as a function of temperature. All data shown are either the result of this work, taken from the data compilation by Irving and Jameison (35), or from Guseinov and Magerramov (27). The only published thermal conductivity data for aqueous organic acids are given by Usmanov (35) at 30 C and Lee (35) at 11 C.

Since the publication of Jameison's thermal conductivity data compilation, Guseinov and Magerramov have published data on the thermal conductivity of pure formic acid.

The formic acid data are given in Tables IV and V, and shown on Figures 9 and 10. The three lines shown represent all of the temperature dependent data. Of these, Guseinov

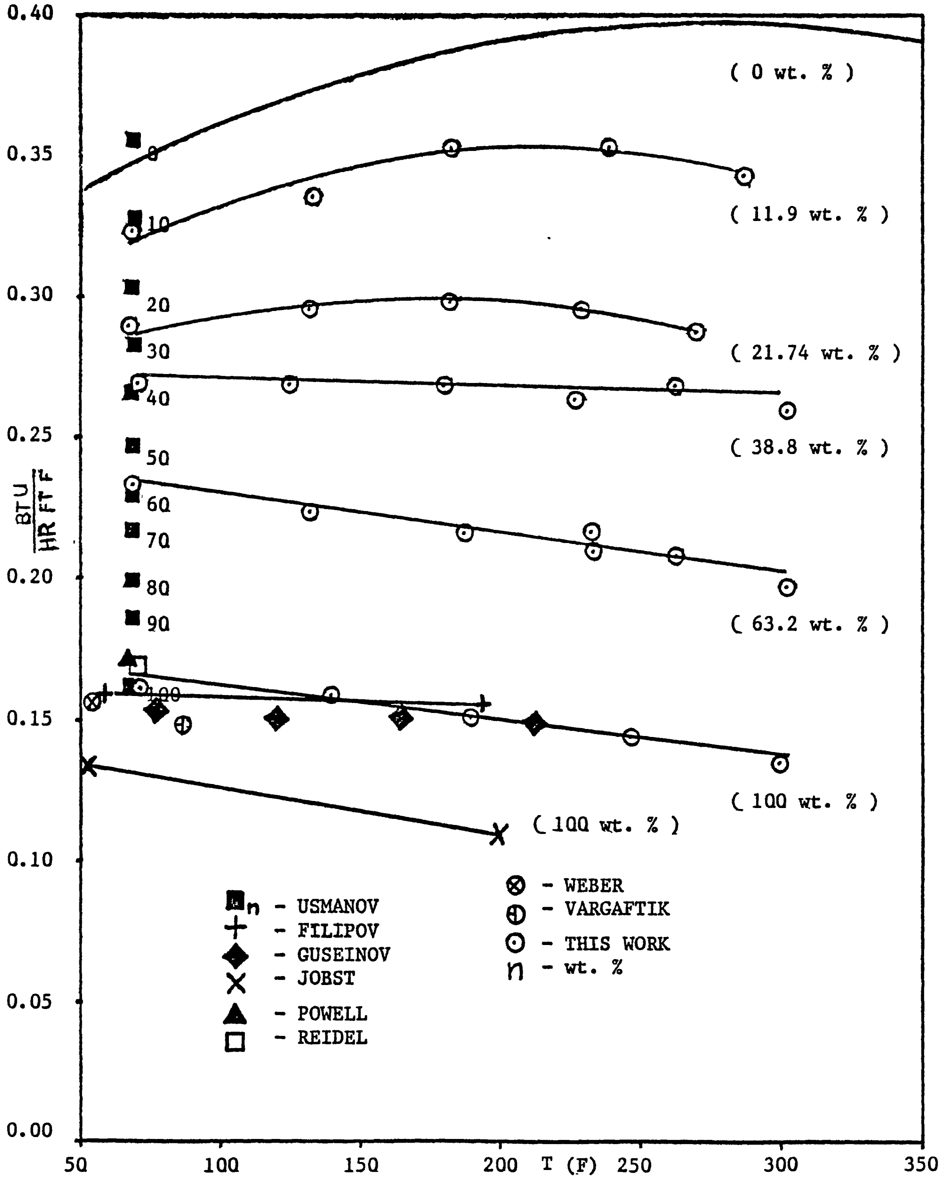

Figure 9. Thermal Conductivity of Aqueous Formic Acid

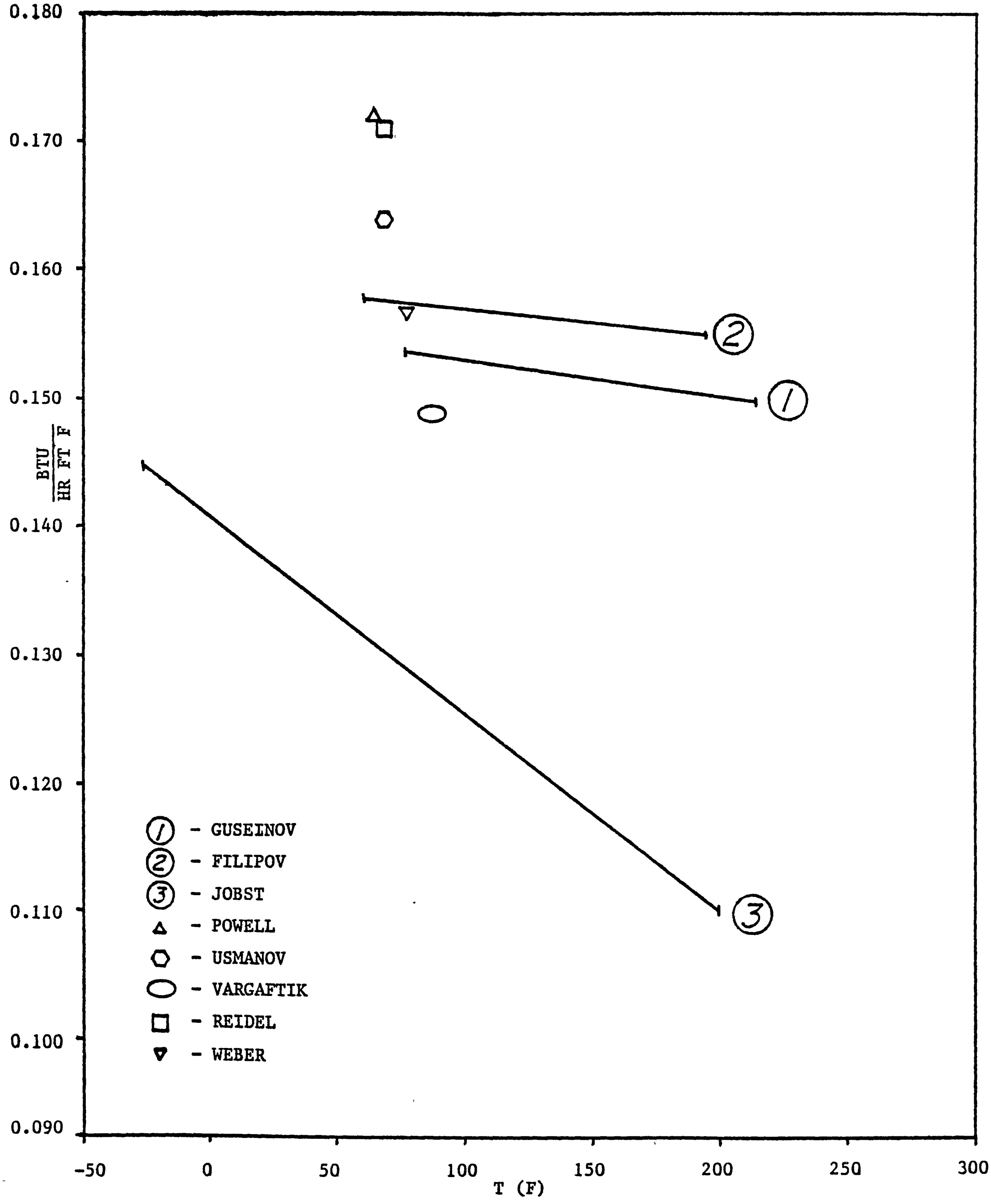

Figure 10. Thermal Conductivity of Pure Formic Acid

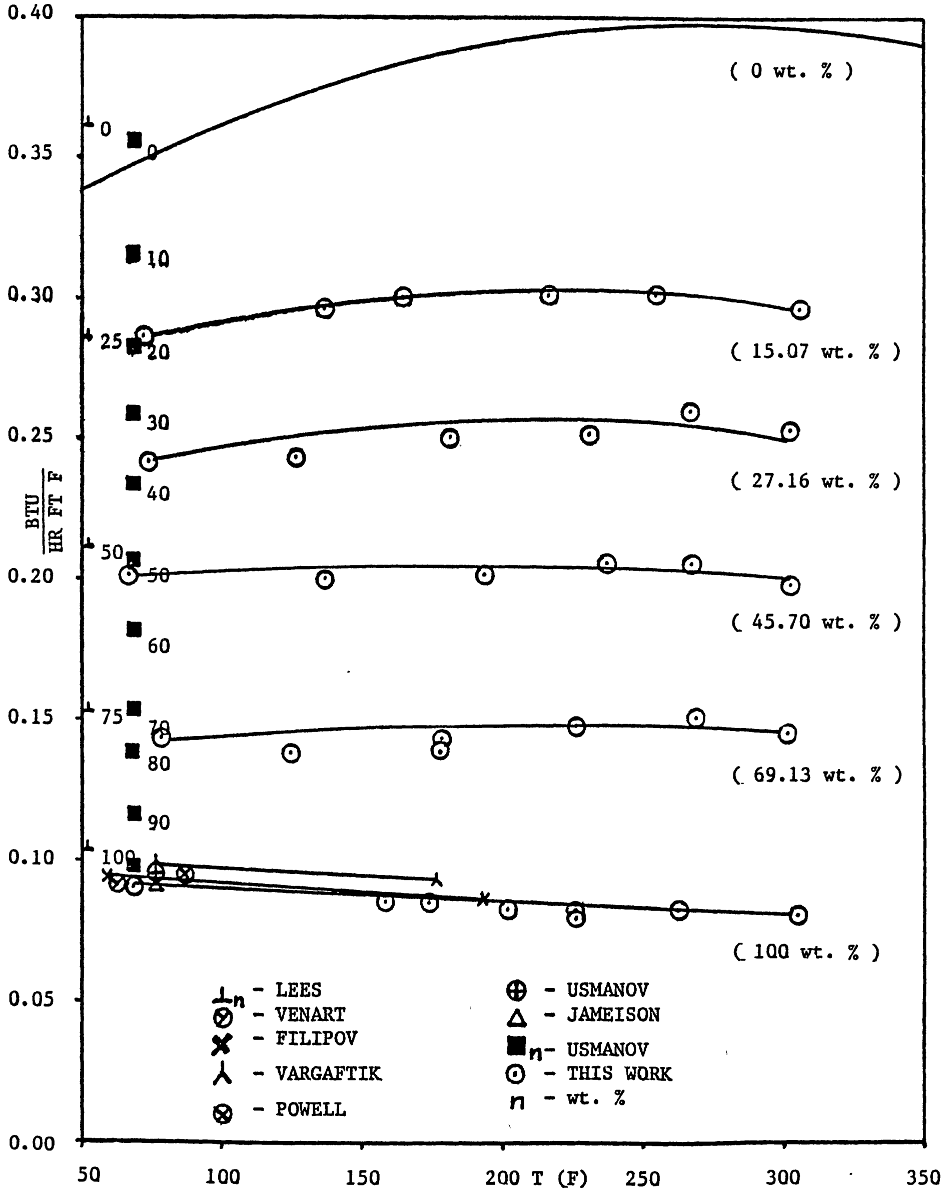

Figure 11. Thermal Conductivity of Aqueous Acetic Acid

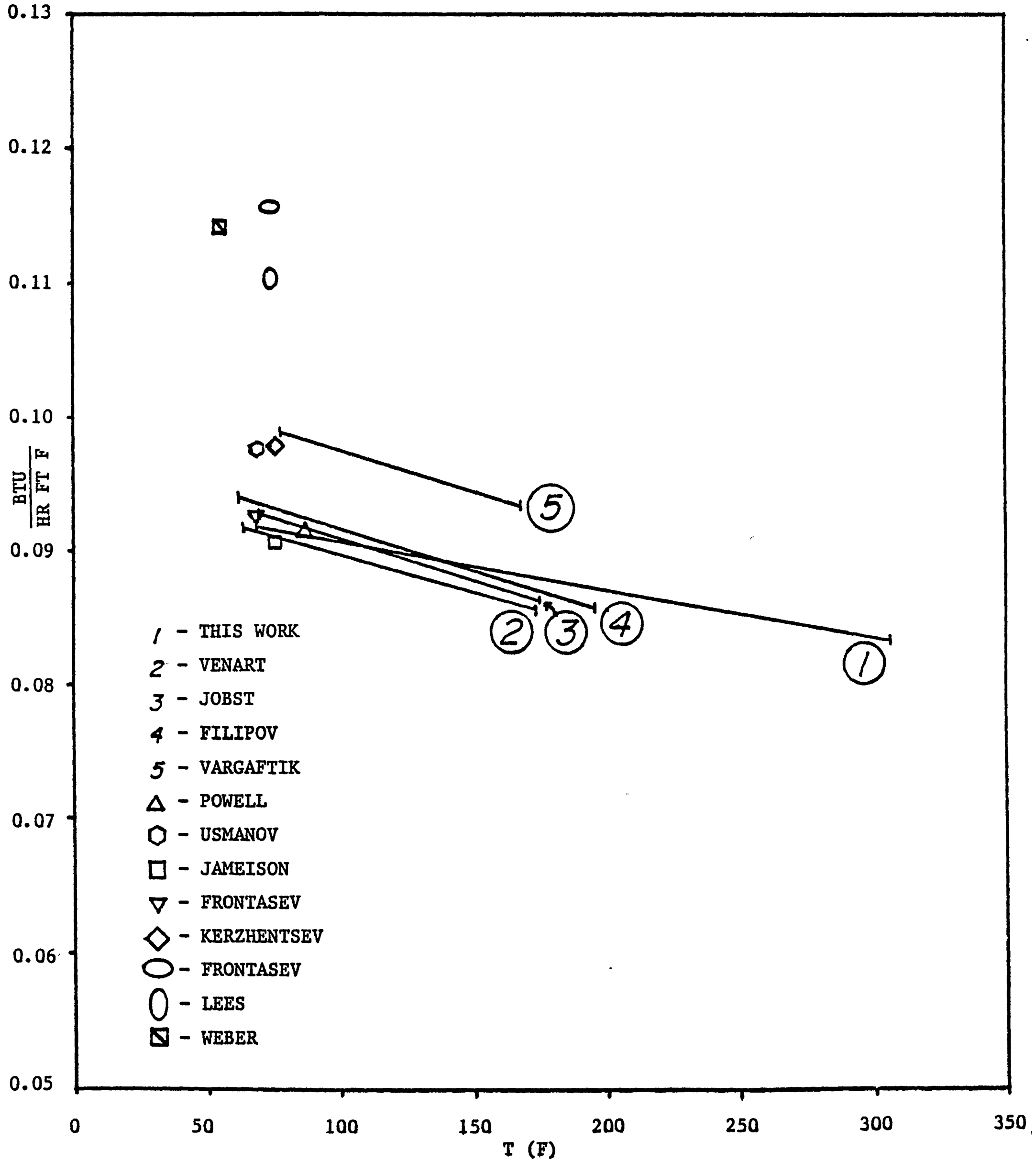

Figure 12. Thermal Conductivity of Pure Acetic Acid

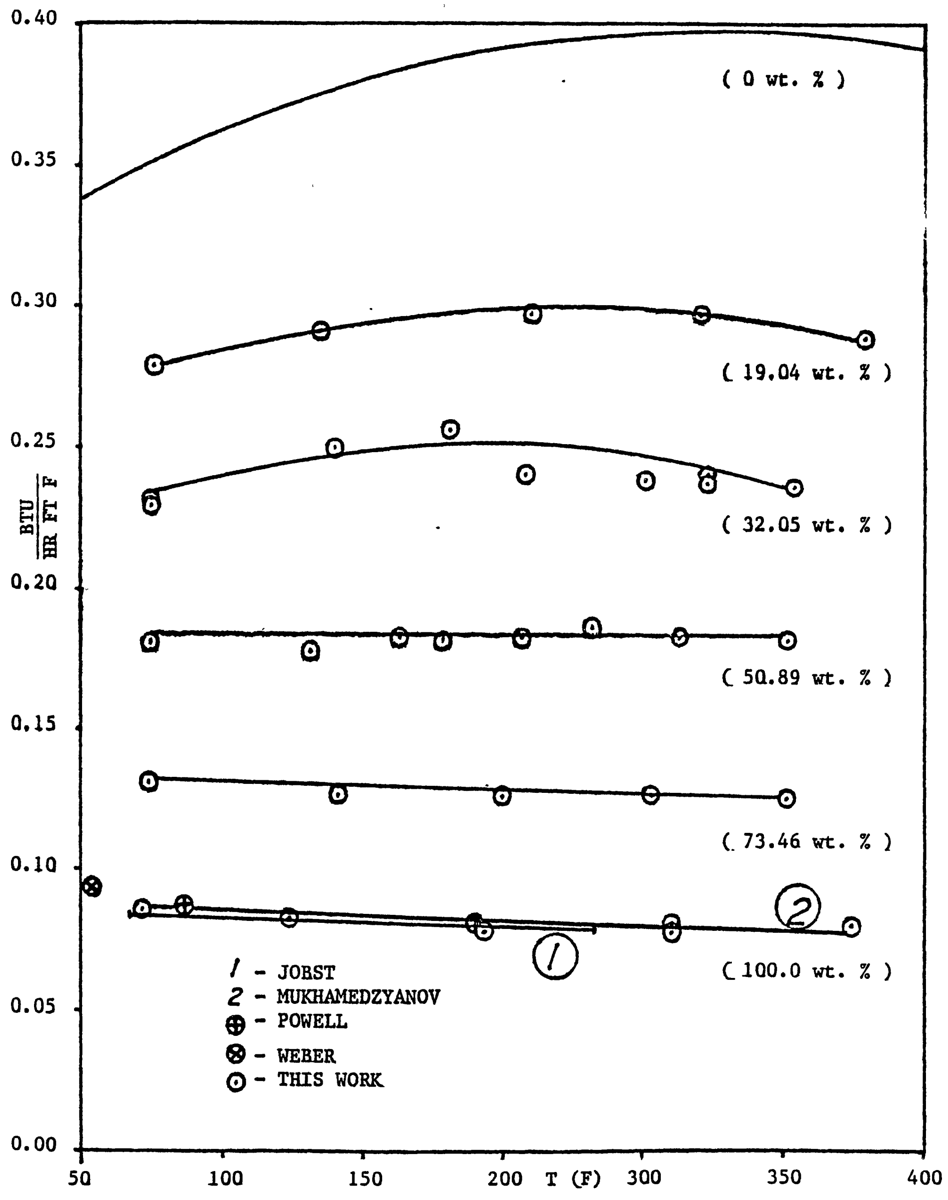

Figure 13. Thermal Conductivity of Aqueous Propionic Acid

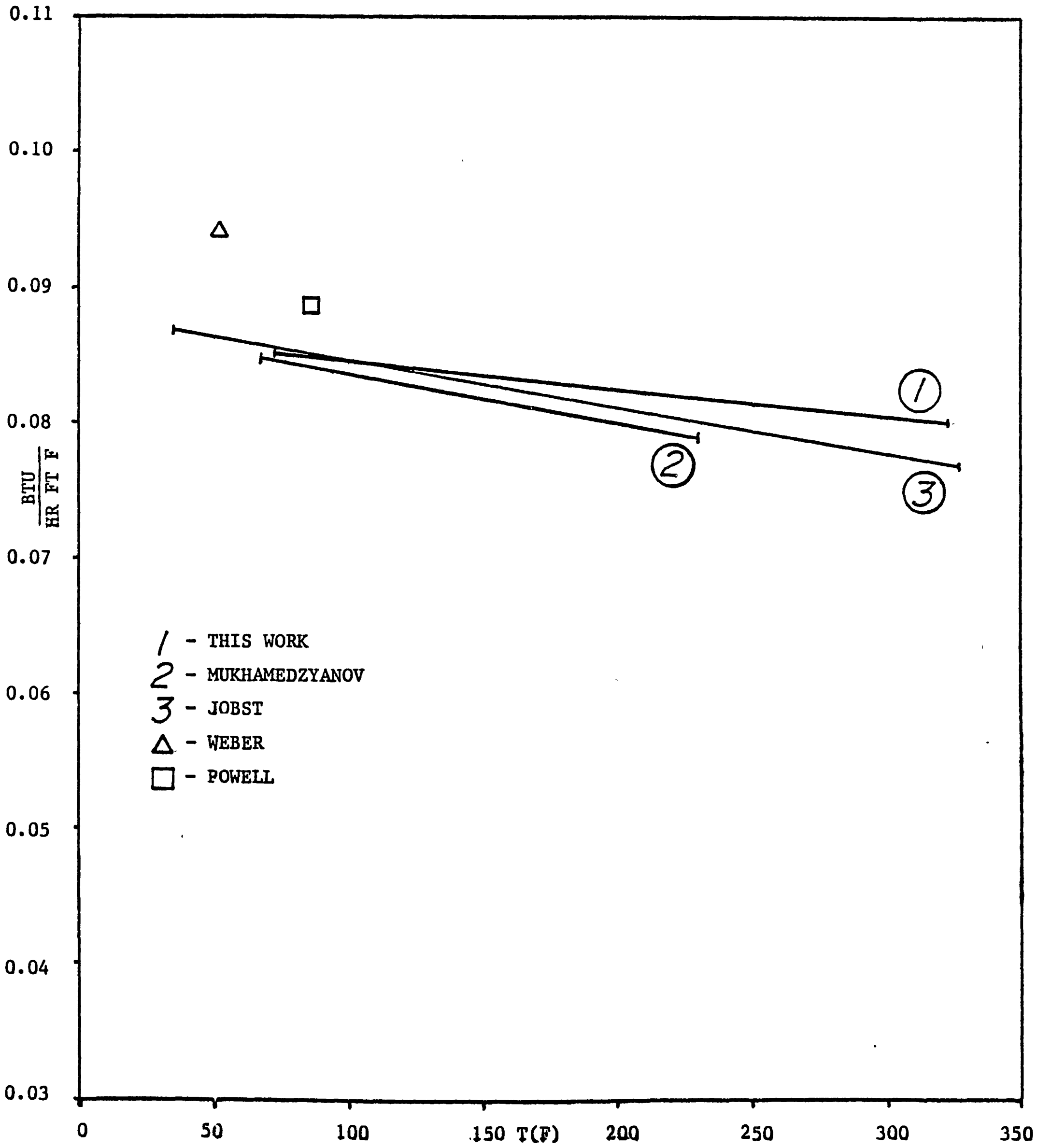

Figure 14. Thermal Conductivity of Pure Propionic Acid

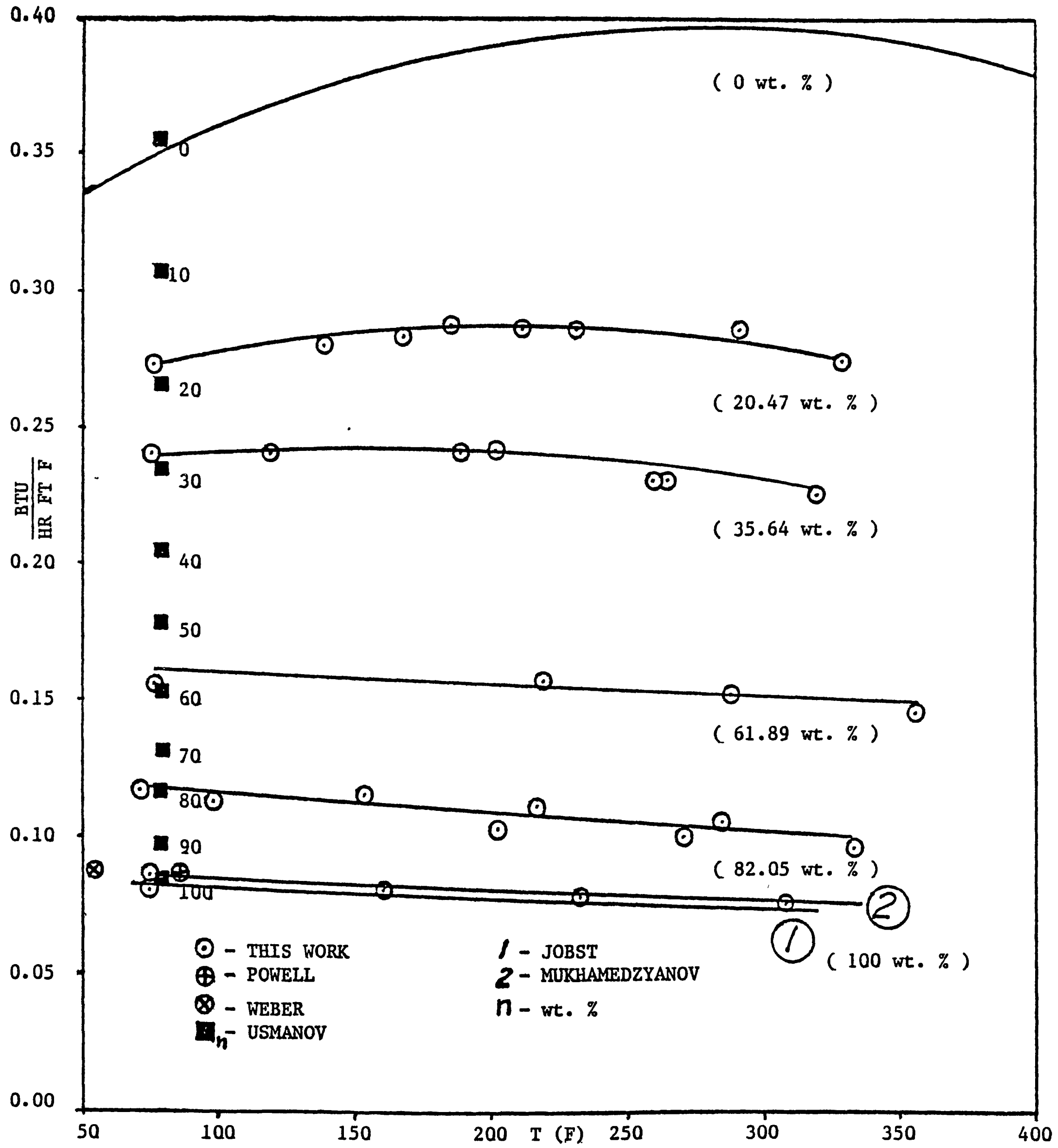

Figure 15. Thermal Conductivity of Aqueous n-Butanoic Acid

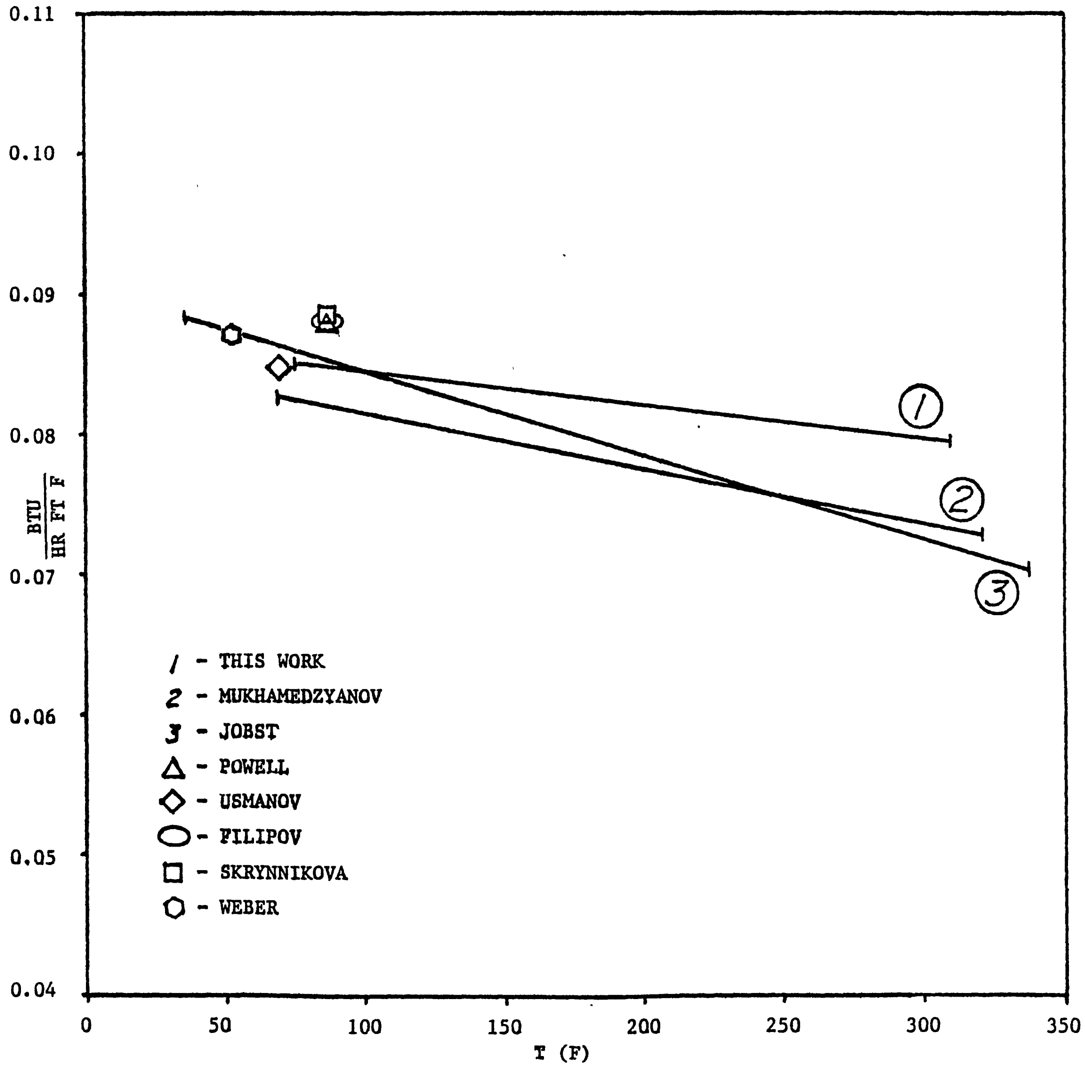

Figure 16. Thermal Conductivity of Pure n-Butanoic Acid

(27) and Filippov (35) agree within 5%, over a temperature range of 77 to 195 F. Jobst's data (35) are lower than those of Guseinov (27) and Filippov (35) by an average of 23% over the temperature range. Also, the temperature dependence of Jobst's data (35) is much more negative than that of the other authors. Single data points presented by Powell (35), Usmanov (35), Vargaftik (35), Reidel (35), and Weber (35) differ by +10% to -5% from the data given by Guseinov (27) and Filippov (35). Pure formic acid was not measured in this work because it degrades at room temperature, producing principally water and carbon monoxide. Pressure build-up is dangerous in storage containers, especially bottles. Water inhibits the reaction, making weaker solutions stable up to 150 C (20). Therefore, only 89.0 wt.% or weaker formic acid was measured. The rate of decrease in thermal conductivity as a function of temperature of data given here is less than that of Jobst (35) but greater than those given by Guseinov (35) and Filippov (35), as shown in given by Jobst (35), Guseinov (35) and Filippov (35), as shown in Figure 9. If the 89.0% formic acid data in this work were extrapolated to pure formic acid, the data in this work would be approximately 4% below that given by Guseinov.

In comparison to the aqueous data presented by Usanov, data shown here for 89.0% formic acid are approximately 13% lower at 30 C. The other aqueous formic acid data given here near 30 C agrees to within 5% of the data presented by Usmanov (35), and are neither consistently lower or higher.

The acetic acid data from this work are given in Table VI and shown on Figure 11. Pure acetic acid data are given in Table VII and shown on Figure 12. The temperature dependent data of Venart (35), Jobst (35), Filippov (35), and this work all agree within 4% over the temperature range shown. Temperature dependent data given by Vargaftik (35) are 5 to 7% higher than these. Several single temperature data points are shown in the range of 50 to 90 F. Three points, by Frontasev (35), Powell (35), and Jameison (35) lie in the range of data given by this work, Venart (35), Jobst (35), and Filoppov (35). Data by Usmanov (35) and Kerzhentsev (35) agree within 2% of the data presented by Vargaftik (35). Data given by Lees (35), Weber (35), and Frontasev (35) in an earlier work average 20% higher than those given in this work. The temperature coefficient of the pure data of this work is less negative than given by either Venart (35), Jobst (35), Filippov (35), or Vargaftik (35). Usmanov's data (35) appear consistently high by 5 to 8% when compared to this work.

The data for propionic acid obtained in this work are given in Table VIII and shown on Figure 13. Data for pure propionic acid are given in Table IX and shown on Figure 14. The temperature dependent data of this work, Mukhamedzyanov (35), and Jobst (35) all agree within 4% over a mutual temperature range. Single temperature points by Powell (35) and Weber (35) are 4 and 10 percent higher, respectively, than determined by this work. No aqueous propionic acid data are available in the open literature.

The data for n-butanoic acid obtained in this work are given in Table X and shown in Figure 15. Data for pure n-butanoic acid is given in Table XI and shown in Figure 16. The data of Mukhamedzyanov (35) and Jobst (35) agree within 5% over a mutual temperature range of 68 to 320 F. Data from this work are within 5% of the data given by Mukhamedzyanov (35) and Jobst (35) to 250 F. At 300 F, these data are 6 and 7% higher than that given by Mukhamedzyanov (35) and Jobst (35), respectively. Single data points obtained by Powell (35), Usmanov (35), Filippov (35), Skrynnikova (35), and Weber (35) all agree within 5% with the data from this work. The aqueous n-butanoic acid data given here are approximately 2 to 5% higher than that given by Usmanov (35).

This work contains the only thermal conductivity data for aqueous organic acids as a function of composition and temperature known to this author. The nature of the data can only be compared qualitatively to data of similar aqueous solutions. Bohne et al (10) have published thermal conductivity data for aqueous ethylene glycol over a similar range of temperature and composition. Their data also show thermal conductivity maxima as a function of temperature. However, Their maxima are somewhat more pronounced than the maxima measured in this work. Arutyunyan and Sarkisyan (6) have published thermal conductivity data for aqueous n-propyl alcohol over a wide range of temperature for concentrations of 25, 50, and 75 wt.%. Their data show weak maxima as a function of temperature, with the maxima disappearing as the water content decreases, which is the same behavior found for the data given in this work.

CHAPTER XIII

CONCLUSIONS AND RECOMMENDATIONS

Conclusions

Previous to this work, relative transient measurements of thermal conductivity were extrapolated to zero time by measuring the initial slope of the hot-wire response to an imposed step voltage. As shown here, both mathematically and empirically, that practice is incorrect, and includes the factor of thermal diffusivity in the measurement. The factor of thermal diffusivity was eliminated from the thermal conductivity measurement by taking the slope measurements on the X-Y recorder at 0.5 second after power was applied.

The basic design of this apparatus along with the modifications made reduced or eliminated several sources of potential measurement error. Radiation and convection heat transfer were eliminated due to the general design of the apparatus. Proper choice of the calibration liquid and time for measurement of the slope of the X-Y recorder output removed error caused by thermal diffusivity. Modifications to the decade resistor arm of each bridge permitted perfect balancing of bridges, eliminating bridge imbalance errors from the measurement and/or reducing time to achieve perfect balance. The improved cell design made the sample cell easy to fill and use, extended the useful temperature range, permitted measurement of more corrosive chemicals, and eliminated strain induced voltage effects from the measurements.

The accuracy of the data given here is estimated to be ±3.5 %, of which ±2 % is attributed to uncertainty in the thermal conductivity of water. The thermal conductivity of water is probably known to better than 2%, but 2% represents a conservative estimate.

The results of this work and the data presented by most other authors generally agree within 5%, which is acceptable for measurements of thermal conductivity. This work presents the only thermal conductivity data for aqueous organic acids over a wide range of temperature. Comparison of the aqueous data of this work to the limited published aqueous data shows adequate to good agreement.

Recommendations

The speed and relative simplicity of the hot-wire apparatus presented in this work, along with the accuracy of the results, commends this method for further study of liquid thermal conductivity, especially for water solutions. The following recommendations are offered for improving the accuracy of the results and productivity of the apparatus:

1. Replace all normal switches in the apparatus with low

resistance gold plated switches.

2. Measure the slope of the X-Y recorder both manually and electronically at the preset time. Agreement between both measurements removes human error in the slope measurements.

3. Construct more measurement cells and add a switch to the test cell bridge so that the thermal conductivity of several liquids can be measured alternately during the same time period. The time for reaching thermal equilibrium is much longer than the time needed for measuring the thermal conductivity of a liquid at equilibrium.

SELECTED BIBLIOGRAPHY

1. Aleksandrov, A.A., and Matveev, A.B., Teploenergetika, 25 (8): 80-85 (1978).

2. Alhabdan, F.A., and Maddox, R.N., Private Communication.

3. Allen, Philip B., Physics Teacher, 21: 582-587 (1983).

4. Alloush, A., Gosney, W.B., and Wakeham, W.A., Int. J. of Thermophysics, 3 (3):225-235 (1982).

5. Amirkhanov, Kh. I., Adamov, A.P., and Magomedov, U.B.,Teplofizika Vysokikh Temperatur, 13 (1): 89-93 (1975).

6. Arutyunyan, G.S., and Sarkisyan, A., Doklady Nauk SSSR, 274 (4): 833-836 (1983).

7. Backstrom, G., J. Phys. E: Sci. Instru., 15: 1049-1053 (1982).

8. Baroncini, C., Di Filippo, P., and Pacetti, M., Int. J. of Thermophysics, 1 (2): 159-175 (1980).

9. Bird, R.B., Stewart, W.E., and Lightfoot, E.N., Transport Phenomena, John Wiley & Sons, Inc., New York, (1960).

10. Bohne, D., Fischer, S., and Obermier, E., Ber. Bunsenges. Phys., Chem., 88: 739-742 (1984).

11. Brasted, Robert C., Comprehensive Inorganic Chemistry, 8, D. Van Nostrand Co., New York (1961).

12. Brueckner, K.A., and Jorna, S., Phys. Rev. Lett., 17 (2): 78-81 (1966).

13. Bushnell, D., and Skogh, J., AIAA Journal, 17 (3): 288-295 (1979).

14. Calmettes, P., and Laj, C., Phys. Rev. Lett., 27 (5): 239-242 (1971).

15. Carslaw, H.S. and Jaeger, J.C., Conduction of Heat in Solids, 2nd. ed., Oxford University Press, New York (1959).

16. Chase, J. David, Chem. Eng. Mag., 107-112, (March 24, 1980).

17. Eatough, D.J., Thermo. Acta, 3: 333-336 (1972).

18. Gebhart, Benjamin, Heat Transfer, 2nd ed., McGraw-Hill Book Co., New York (1971).

19. Geller, V.Z., Paramonov, I.A., and Tatevosov, G.D., Fluid Mech. Sov. Res., 3: 109-113 (1974).

20. Giglio, M., and Vendramini, A., Appl. Phys. Lett., 25 (10): 555-557 (1974).

21. Gil'bird, M.M., Moin, F.B., Pazderskii, Yu.A., Zadvornyak, V.D., and Yurkevich, B.N., J. Appl. Chem. USSR, 57 (4): 851-852 (1984).

22. Goldner, F.J., Int. J. Heat and Mass Trans., 21: 69-73 (1978).

23. Golubev, I.F., Teploenergetika, 10: 78 (1963).

24. Gordon, J.P., Leite, R.C.C., Moore, R.S., Porto, S.P.S., and Whinnery, J.R., J. Appl. Phys., 36 (1): 3-8 (1965).

25. Grishchenko, A.E., and Grishchenko, G.V., Zhur. Prikl. Khim., 52 (2): 308-311 (1983).

26. Gurenkova, T.V., Norden, P.A., and Usmanov, A.G., Fluid Mech. Sov. Res., 3: 114-118 (1974).

27. Guseinov, K.D., and Magerramov, S.G., Russ. J. Phys. Chem., 48 (3): 332-334 (1974).

28. Head, J.S., Johnson, R.C., and Maddox, R.N., Private Communication.

29. Healy, J.J., de Groot, J.J., and Kestin, J., Physica C, 82C: 392-408 (1976).

30. Horrocks, J.K., and McLaughlin, E., Trans. Farad. Soc., 58: 1357 (1962).

31. Hu, C., and Whinnery, J.R., Appl. Optics, 12 (1): 72-79 (1973).

32. Int. Assoc. Prop. Steam, Eighth Int. Conf., (1974).

33. Irving, J.B., and Jameison, D.T., Thermal Conductivity Measurement by an Improved A.C. Hot-Wire Method, Nat. Eng. Lab., Dept. of Industry, Glasgow, England (1976).

34. Jameison, D.T., and Hastings, E.H., The Thermal Conductivity of Binary Liquid Mixtures, The Eighth Conference on Thermal Conductivity, Purdue Research Foundation, 631-641 (1969).

35. Jameison, D.T., Irving, J.B., and Tudhope, J.S., Liquid Thermal Conductivity: a Data Survey to 1973, Edinburgh, Scotland, (1975).

36. Jameison, D.T., and Tudhope, J.S., Desal. 8: 393-401 (1970).

37. Kirk-Othmer Encyclopedia of Chemical Technology, 3rd. ed., John Wiley & Sons, New York, 13: 337-343 (1981).

38. Koren, G., Phys. Rev. A, 13 (3): 1177-1184 (1976).

39. Lagar'kov, A.N., and Sergeev, V.M., Teplofizika Vysokikh Temperatur, 11 (6): 1162-1168 (1973).

40. Lalanne, J., Pouligny, B., and Sein, E., J. Phys. Chem., 87 (4): 696-707 (1983).

41. Lee, M.C. and Maddox, R.N., Private Communication.

42. Leidenfrost, W., Measurements of Thermal Conductivity of Toluene, School of Mech. Eng., Heat Transfer Lab., Purdue Univ, Indiana (1975).

43. Leite, R.C.C., Moore, R.S., and Whinnery, J.R., Appl. Phys. Lett., 5 (7): 141-143 (1964).

44. Le Neindre, B., Bury, P., Tufeu, R., and Vodar, P., J. Chem. Eng. Data, 21 (3): 265-274 (1976).

45. Li, C.C., AIChE Journal, 22 (5): 927-930 (1976).

46. Maddox, R.N., Private Communication.

47. Madzhidov, Kh., and Safarov, M.M., Russ. J. Phys. Chem., 58 (1): 28-30 (1984).

48. Mallan, G.M., Marshall,S., and Lockhart,F.J., J. Chem. Eng. Data, 17 (4): 412-415 (1972).

49. Mathur, V.K., Lilly, L.L., and Maddox, R.N.,

Private Communication.

50. Menashe, J., and Wakeham, W.A., *Int. J. of Heat and Mass Trans.*, *25* (5): 661-673 (1982).

51. Miller, G.L., *Metallurgy of the Rarer Metals*, *6*: *Tantalum and Niobium*, ed. by H.M. Finniston, Academic Press, New York, 1959.

52. Nagasaka, Y., and Nagashima, A., *J. Phys. E: Sci. Instru.*, *14*: 1435-1439 (1981).

53. Nangia, K.K., and Chenoweth, J.M., *Thermal Conductivity Apparatus Data Book*, Heat Transfer Research Inc., unpub. (1972).

54. Nietro de Castro, C.A., Calado, J.C.G., Wakeham, W.A., and Dix, M., *J. Phys. E*, *9*: 1073-1076 (1976).

55. Nietro de Castro, C.A., Fareleira, J.M.N.A., and Calado, J.C.G., *Proceedings of the Eighth Symposium on Thermophysical Properties*, *ASME Publications*, *1*: 247-249 (1982).

56. *Niobium*, *Tantalum*, *Molybdenum*, *and Tungsten*, ed. by A.G. Quarrell, Elsevier Pub. Co., New York (1961).

57. Ogiwara, K., Arai, Y., and Saito, S., *J. Chem. Eng. Japan*, *15* (5): 335-342 (1982).

58. Pearson, Carl E., *Handbook of Applied Mathematics Selected Results and Methods*, Van Nostrand Reinhold, New York, 344-377 (1974).

59. Phylippov, L.P., Nefedov, S.N., and Kravchoon, S.N., *Int. J. of Thermophysics*, *1* (2): 141-146 (1980).

60. Pouchert, Charles J., *The Aldrich Library of Infrared Spectra*, 3rd. ed., Aldrich Chemical Co., Milwaukee, Wisconson (1981).

61. Powell, R.W., and Groot, H., *Int. J. of Heat and Mass Transfer*, *15*: 360-366 (1972).

62. Raal, J.D., and Rijsdijk, R.L., *J. Chem. Eng. Data*, *26*: 351-359 (1981).

63. Rastoguev, Yu.L., and Ganiev, Yu.A., *Russ. J. Phys. Chem.*, *41* (6): 717 (1967).

64. Roder, H.M., *J. Res. Nat. Bur. Stand.*, *86* (5):

457-493 (1981).

65. Saksena, M.P., and Harminder, Chem. Phys. Lett., 27 (3): 448-450 (1974).

66. Saksena, M.P., and Harminder, Chem. Phys. Lett., 25 (3): 445-448 (1974).

67. Saksena, M.P., and Harminder, Ind. Eng. Chem. Fund., 13 (3): 245-247 (1974).

68. Schrock, V.E., and Starkman, E.S., Rev. Sci. Inst., 29: 625 (1958).

69. Shroff, G.H., Measurement and Correlation of Thermal Energy Transport in Non-Ideal Binary Liquid Systems, The Eighth Conference on Thermal Conductivity, Purdue Research Foundation, 643-658 (1969).

70. Sisco, Frank T. and Epremian, Edward, Columbium and Tantalum, John Wiley & Sons, New York (1963).

71. Skinner, D.R., Optics Communications, 1 (2): 57-58 (1969).

72. Skripov, V.P., and Galashev, A.E., Russian Chemical Reviews, 52 (2): 97-116 (1983).

73. Solimini, D., J. Appl. Phys., 37 (2): 3314-3315 (1966).

74. Tada, Y., Harada, M., Tanigaki, M., and Eguchi, W., Ind. Eng. Chem. Fund., 20 :333-336 (1981).

75. Thermal Conductivity, ed. by R. P. Tye, Academic Press, New York, 2 (1969).

76. Thermophysical Properties of Matter, 3: Thermal Conductivity, Non - Metallic Liquids and Gases, ed. by Y.S. Touloukian, IFI/Plenum, New York, 3a-21a (1970).

77. Thermophysical Properties of Matter, 6: Specific Heat, Non - Metallic Liquids and Gases, ed. by Y.S. Touloukian, IFI/Plenum, New York (1970).

78. Tsederberg, N. K., Thermal Conductivity of Gases and Liquids, M.I.T. Press, Cambridge, Mass. (1965).

79. Tufeu, R., Ivanov, D.Y., Garrabos, Y., and Le Neindre, B., Ber. Bunsenges. Phys. Chem., 88:

422-427 (1984).

80. Uhlig, Herbert H., The Corrosion Handbook, John Wiley & Sons, New York, 323 (1948).

81. Usmanov, I.U., and Salikhov, A.S., Russ. J. Phys. Chem., 51 (10): 1488-1489 (1977).

82. Van Loef, J.J., Physica A, 87A: 258-272 (1977).

83. Vilcu, R., Ciochina, A., and Vasu, Gh., Revue Roumaine de Chimie, 26: 1355-1364 (1981).

84. Yaws, C.I., Chem. Eng., Oct. 25: 127-135 (1976).

APPENDIX A

DERIVATION OF HOT WIRE THERMAL CONDUCTIVITY EQUATION

The measurements taken in this work are not direct measurements of thermal conductivity. The apparatus measures the change in resistance of both the test and reference filament caused by an increase in temperature of the filament. Direct current electrically heats the wire while the wire is cooled by the surrounding liquid. The greater the thermal conductivity of the liquid, the slower the wire heats at a given applied current.

The filament is mathematically modeled as a line source. Heat conduction into the liquid in only the radial direction is assumed, and convection heat transfer is not considered. The basic equation for describing this mathematically is given by Bird et al (9).

$$\rho C_V \, (\partial T/\partial t) = -1/r \, [\partial/\partial r \, (r q_r)] \qquad \text{(AI.1)}$$

The heat flux term is related to the fluid thermal conductivity by:

$$q_r = - \lambda \, \partial T/\partial r \qquad \text{(AI.2)}$$

A step change in voltage on each filament produces a step change in heat output at the wire surface. The boundary and initial conditions are:

$$\text{at } r = r_0, \lim_{r \to r_0} (r\partial T/\partial r) = -q_r/2\pi\lambda \qquad (\text{AI.3})$$

$$\text{at } r = \infty+, \lim_{r \to \infty+} \Delta T\ (r,t) = 0 \qquad (\text{AI.4})$$

$$\text{at } t = 0, T\ (r,t) = 0 \qquad (\text{AI.5})$$

The first condition requires that the surface heat flux be at steady state. The second and third conditions require the system to be everywhere in thermal equilibrium.

For liquids at low to moderate pressure, the constant volume and constant pressure heat capacity are effectively equal. Since constant pressure heat capacity data are more available than constant volume heat capacity data, the former will be used in place of the latter.

Equations AI.1 and AI.2 can be combined to give;

$$\rho C_p\ (\partial T/\partial t) = -\lambda\ (\partial^2 T/\partial r^2) - \lambda/r\ (\partial T/\partial r) \qquad (\text{AI.6})$$

In terms of thermal diffusivity, equation AI.6 becomes;

$$(\partial T/\partial t) = -\alpha\ (\partial^2 T/\partial r^2) - \alpha/r\ (\partial T/\partial r) \qquad (\text{AI.7})$$

LaPlace transforms are conveniently used to solve the above equation, where both the factors of time and radial distance determine the temperature distribution of the fluid. The definition of the LaPlace transform is;

$$\pounds \{T(r,t)\} = \bar{t} = \int_0^\infty \exp\,(-pt\;(r,t))\;dt \qquad (AI.8)$$

where "p" is a positive number, large enough to force the stated integral to converge. Some useful LaPlace transforms required to transform equation AI.7 are:

$$\pounds \{\partial T/\partial t) = p\pounds\{T\} - T_0,\; T_0 = \lim_{t \to 0} (T) \qquad (AI.9)$$

$$\pounds\, [\partial^n T/\partial r^n\} = d^n\bar{t}/dr^n \qquad (AI.10)$$

The LaPlace transform of equation AI.7 is

$$d^2\bar{t}/dr^2 + 1/r(d\bar{t}/dr) - p/\alpha\;(\bar{t}) = 0 \qquad (AI.11)$$

letting,

$$s^2 = p/\alpha \qquad (AI.12)$$

equation AI.11 becomes;

$$d^2\bar{t}/dr^2 + 1/r\;(d\bar{t}/dr) - s^2\,\bar{t} = 0 \qquad (AI.13)$$

which is a modified Bessel equation. Its general form is;

$$d^2Y/dz^2 + 1/z\;(dY/dz) - (1 - \nu^2/x^2)Y = 0 \qquad (AI.14)$$

and its general solution is;

$$I_\nu(z) = \sum_{n=0}^{\infty} (z/2)^{\nu+2n}/[n!\ \Gamma(\nu + n + 1)] \qquad \text{(AI.15)}$$

such that;

$$K_\nu(z) = \pi/2\ [I_{-\nu}(z) - I_\nu(z)]/\sin\nu\pi \qquad \text{(AI.16)}$$

The boundary conditions in terms of the LaPlace variable are;

$$\text{at } r = r_0,\ \overline{t} = q/\lambda \qquad \text{(AI.17)}$$

$$\text{at } r \to \infty+,\ \overline{t} \text{ is finite} \qquad \text{(AI.18)}$$

Since,

$$K_0'(z) = -K_1(z) \qquad \text{(AI.19)}$$

and;

$$\mathcal{L}\{\textstyle\int_0^t v(t')\,dt'\} = 1/p\ \mathcal{L}\{v\} \qquad \text{(AI.20)}$$

the general solution of the LaPlace transform for equation AI.14 is;

$$\overline{t} = qK_0(sr)/\lambda p s K_1(sr_0) \qquad \text{(AI.21)}$$

The generalized La Place transform inversion formula is;

$$T(t) = \frac{1}{2\pi i} \int_{\gamma - i\infty}^{\gamma + i\infty} \exp\ (\varepsilon t)\ \overline{t}\ (\varepsilon)\ d\varepsilon \qquad \text{(AI.22)}$$

allowing;

$$\mu = (\varepsilon/\alpha)^{1/2} \qquad \text{(AI.23)}$$

the solution for temperature in terms of complex Bessel functions follows. These Bessel functions are normally expressed as polynomials including simpler Bessel functions.

$$T = q/2\pi i \int_{-\infty}^{0} [e^{\varepsilon t}\ K_0(\mu r)/(\varepsilon\mu K_1(\mu r))]\ d\varepsilon \qquad \text{(AI.24)}$$

The modified Bessel functions of the first and second order reduced to simpler terms are;

$$K_0(z) = -\ [\{\ell n(z/2) + \gamma\}\ I_0(z) + (z/2)^2 + (3/2)\ (z/2)^4/2! + \ .\ .\ .] \qquad \text{(AI.25)}$$

and;

$$K(z) = (-1)^0\ \{\ln(z/2) + \gamma\}\ I(z) - 1/2\ \{[\sum_{n=0}^{\infty} (z/2)^{2n+1}/(n!(1+n))][\sum_{m=1}^{n+1} m^{-1} + \sum_{m=1}^{n} m^{-1}] \qquad \text{(AI.26)}$$

Therefore,

$$
\begin{aligned}
T = {} & -qr_o/2\pi i\lambda \int_{\infty}^{o} e^{\varepsilon t}/\varepsilon \ \{[\ln (C^* r\mu/2) + (r^2\mu^2/4) \\
& * (\ln(C^* r\mu/2) - 1) + \ldots]/[1 + (\mu^2 r_o^2/2) \\
& * (\ln(C^* r_o\mu/2) - \tfrac{1}{2}) + \ldots]\} \, d\varepsilon
\end{aligned}
\qquad \text{(AI.27)}
$$

which reduces to;

$$
\begin{aligned}
T = {} & qr_o/2\pi i\lambda \int_{-\infty}^{o} e^{\varepsilon t}/\varepsilon \ \{\tfrac{1}{2} \ln (C^{*2} r^2/4\alpha) \\
& + (r^2\varepsilon/8\alpha) \ln(C^{*2} r^2\varepsilon/4\alpha) - r^2\varepsilon/4\alpha - (\varepsilon r_o^2/8\alpha) \\
& * (\ln(C^{*2} r^2 \varepsilon/4\alpha)) - (\varepsilon r_o^2/4\alpha) (\ln (r_o/r) - \tfrac{1}{2}) \\
& * \ln(C^{*2} r^2 \varepsilon/4\alpha) + \ldots\} \, d\varepsilon
\end{aligned}
\qquad \text{(AI.28)}
$$

Use of equation AI.23 gives:

$$
\begin{aligned}
T = {} & qr_o/2\pi i\lambda \int_{-\infty}^{o} e^{\varepsilon t}/\varepsilon \ \{\ln(C^* \mu r/2) \\
& + (r^2\mu^2/4) [\ln(C^* r\mu/2 - 1)] - (r_o^2\mu^2/2) \\
& * [\ln(C^* r\mu/2)] [\ln (C^* r\mu/2) + \ln(r_o/r) \\
& - \tfrac{1}{2}] + \ldots\} \, d\varepsilon
\end{aligned}
\qquad \text{(AI.29)}
$$

The following integrals are used to integrate the above equation by parts. Note that fourth order and higher terms are dropped from equations AI.25 to AI.29.

$$
1/2\pi i \int_{-\infty}^{o} \varepsilon^{-\nu-1} e^{\varepsilon t} \, d\varepsilon = t^{\varepsilon}/\Gamma (1 + \nu) \qquad \text{(AI.30)}
$$

$$
1/2\pi i \int_{-\infty}^{o} \varepsilon^{n} \, e^{\varepsilon t} \, d\varepsilon = 0, \ n = 0, 1, 2, \ldots \qquad \text{(AI.31)}
$$

$$
1/2\pi i \int_{-\infty}^{o} 1/\varepsilon \ e^{\varepsilon t} \ln(K_1\varepsilon) \, d\varepsilon = \ln(C_N t/K_1) \qquad \text{(AI.32)}
$$

$$1/2\pi i \int_{-\infty}^{0} e^{\varepsilon t} [\ln (b\varepsilon)^2] \, d\varepsilon = \frac{2}{t} \ln C_N t/b \qquad \text{(AI.33)}$$

$$1/2\pi i \int_{-\infty}^{0} e^{\varepsilon t} \ln(b\varepsilon) \, d\varepsilon = -1/t \qquad \text{(AI.34)}$$

The following result is obtained from equations AI.29 through AI.34 for the temperature distribution in the fluid.

$$T = qr_0/2\lambda \, \{\ln(4\alpha t/C^* r_0{}^2) + r_0{}^2/4\alpha t + (r_0{}^2/2\alpha t) \\ /(\ln(4\alpha t/C^* r_0{}^2)) + (2r_0{}^2/4\alpha t) \, * \\ * \ln(r_0/r) + \ldots\} \qquad \text{(AI.35)}$$

As discussed in Chapter VI, equation AI.35 simplifies to the following equation for times greater than 0.10 second.

$$T = qr_0/2\lambda \, \ln(4\alpha t/C^* r_0{}^2) \qquad \text{(AI.36)}$$

The recorder pen deflection can be represented by;

$$dy = E_{T_y} \Delta T_y = (G_y/E_{v_y}) \, \Delta V_y \qquad \text{(AI.37)}$$

$$dx = E_{T_x} \Delta T_x = (G_x/E_{v_x}) \, \Delta V_x \qquad \text{(AI.38)}$$

The voltage changes across the unbalanced bridges with respect to the changing resistances are;

$$\Delta V_y = (V_{Br})_y \, / \, (4dR_y/R_y) \qquad \text{(AI.39)}$$

$$\Delta V_x = (V_{Br})_x \,/\, (4dR_x/R_x) \qquad \text{(AI.40)}$$

For small temperature changes, the change in resistance is linear with temperature.

$$dR_y/R_y = A_y dT_y/R_y \qquad \text{(AI.41)}$$

$$dR_x/R_x = A_x dT_x/R_x \qquad \text{(AI.42)}$$

Combining equations AI.38 through AI.42 gives;

$$dy = (G_y/E_{v_y})\ (V_{Br}/4)_y\ A_y\ dT_y/R_y \qquad \text{(AI.43)}$$

$$dx = (G_x/E_{v_x})\ (V_{Br}/4)_x\ A_x\ dT_x/R_x \qquad \text{(AI.44)}$$

The X-Y recorder plots the slope of the combined pen deflections;

$$\Delta y/\Delta x = \tan\Theta \qquad \text{(AI.45)}$$

The temperatue of each filament is related to the heat input and the thermal conductivity of the liquid around it.

$$\Delta T_y = q_y/\lambda_y \qquad \text{(AI.46)}$$

$$\Delta T_x = q_x/\lambda_x \qquad \text{(AI.47)}$$

The heat input to each filament is related to the impressed voltage, and length and resistance of each filament.

$$q_y = (V_{Br})_y^{\,2} \; / \; 4R_y l_y \qquad \text{(AI.48)}$$

$$q_x = (V_{Br})_x^{\,2} \; / \; 4R_x l_x \qquad \text{(AI.49)}$$

Equations AI.36 through AI.49 are combined to give a complete equation.

$$\lambda_y = \lambda_x/\tan\Theta \; \{[(V_{Br})_y/(V_{Br})_x]^3 \; [R_x/R_y]^2 \; * \; (l_x \; G_y \; A_y \; E_{V_x} \; / l_y \; G_y \; A_x E_{V_y}) \; [\ln \; (4\alpha_y t/C^* r_o^{\,2})/ \; \ln \; (4\alpha_x t/C^* r_o^{\,2})]\} \qquad \text{(AI.50)}$$

The terms involving filament length, recorder sensitivity, differential amplifier gain, and resistance temperature coefficient are combined into the calibration constant, giving the following equation.

$$\lambda_y = C_o(T)/\tan\Theta \; \{[(V_{Br})_y/(V_{Br})_x]^3 \; (R_x/R_y)^2 \; * \; [\ln(4\alpha_y t/C^* r_o^{\,2}) \; / \; \ln(4\alpha_x t/C^* r_o^{\,2})]\} \qquad \text{(AI.51)}$$

Since the above equation for thermal conductivity is a function of thermal diffusivity, it can be solved only by trial and error.

As shown in Chapter VI, at times less than approximately 0.4 second, the thermal diffusivity of the liquid being measured can alter the measurement. In this work, the measurement time was 0.5 second, which eliminated the effect of the liquid thermal diffusivity, assuring that only the thermal conductivity of the fluid was being measured. The final working equation is obtained by dropping the term containing the thermal diffusivity and substituting the test cell and reference cell indices for the indices y and x, respectively.

$$\lambda_y = C_o(T)/\tan\Theta \{[V_t/V_r]^3 [R_r/R_t]^2\} \qquad (AI.52)$$

APPENDIX B

ERROR ANALYSIS

The sources of error in this work are due to: effects discussed in Chapter XI, accuracy and reproducibility of the electronic equipment, and accuracy in reading the slope of the line produced by the electronic equipment. Negligible error can be attributed to solution preparation and temperature measurements.

The millivolt potentiometer allowed temperature measurement to within 0.05 F without reading between divisions. No further accuracy was needed for measuring the overall absolute system temperature.

The differential gain accuracy of 0.1% contributes a maximum of 0.2% error to the output, which is the slope on the X-Y plotter. This has a direct effect on the final value for thermal conductivity.

The voltmeters, with a resolution of 1 millivolt, contribute a maximum error of 2 millivolts. The accuracy of these meters was not a factor, as the calibration of the test cell would include any systematic accuracy error into the calibration constant.

The accuracy of the decade resistors was not a contributing factor either, as it would enter as a factor into the calibration constant of the test cell. However, the variable potentiometers, which were allowed to vary the resistance of the test cell by no more than 0.01 ohm, could contribute up to 0.02 ohm error.

The solutions were prepared from reagent grade acids on a balance accurate to 0.001 gram. The solutions were prepared according to their reported acid content with respect to the reported water or anhydride content. Accuracy of the solution concentrations was at least to within 0.02% for acetic, propionic, and n-butanoic acids, and 0.1% for formic acid. As the thermal conductivity of these solutions is not a strong function of acid concentration, error due to preparation of the solutions is less than 0.01%.

From the form of equation 9.1, with representative average values of voltage and resistance for a measurement of 2.000 volts and 30.00 ohms, the maximum error contributed by voltage and resistance errors is given by:

$$\begin{aligned} \text{error} &= 1 - (30.01/29.99)(2.001/1.999) \qquad (\text{AII.1}) \\ &= 0.0043 \end{aligned}$$

which gives a representative uncertainty of 0.43%.

The slope of the X-Y recorder line was measured manually. A straight edge was used to extend the slope of the linear section of the output, taken at 0.5 seconds, to the limits of the graph paper. The graph was resolved into blocks of 0.05 inches. The slope could be read to ±0.01 inches on both axes. The length of the line drawn projected on each axis was usually 4 to 6 inches. The maximum uncertainty error contributed to the thermal conductivity by manually reading the slope is 0.50%. Uncertainty due to inexactly determining the slope, which cannot be calculated, probably did not exceed 0.5%.

The total maximum uncertainty error is approximately 1.5%. Reproducibility of data was within ±1%. The reported uncertainty in the calibration fluid data averages 2.0% (5,35,75), making the accuracy of the data reported in this work within ±3.5%.

APPENDIX C

RADIATION CALCULATION

The radiant contribution of heat transfer to the measurement for a thermally transparent liquid follows the Stefan-Boltzmann equation.

$$Q_{rad} = 2\pi r_o \sigma \, (T_1{}^4 - T_w{}^4) \qquad \text{(AIII.1)}$$

The radius of the hot-wire is 0.0013 cm, or 0.000013 meters. For a fluid temperature of 450 K (350 F) at thermal equilibrium, and the temperature rise of 0.23 K found in this work for both filaments during measurement, the above equation is evaluated.

$$\begin{aligned} Q_{rad} = {} & 2 * 3.14159 * 0.000013\text{m} * 5.67 * 10^{-8} \\ & \text{W/m}^2\text{K}^4 * ((450.23 \text{ K})^4 - (450 \text{ K})^4) \end{aligned} \qquad \text{(AIII.2)}$$

$$\begin{aligned} Q_{rad} &= 4.63 * 10^{-12} * 8.39 * 10^7 \\ &= 3.88 * 10^{-4} * \text{W/m} \end{aligned} \qquad \text{(AIII.3)}$$

For a fluid temperature of 300 K (80 F), the radiant contribution would be;

$$\begin{aligned} Q_{rad} &= 4.63 * 10^{-12} * ((300.23 \text{ K})^4 - (300 \text{ K})^4) \\ &= 1.15 * 10^{-4} \text{ W/m} \end{aligned} \qquad \text{(AIII.4)}$$

The electrical heating equation for any wire is:

$$Q_{el} = (V^2/R)\Delta t \tag{AIII.5}$$

The duration of each measurement was 0.50 second. The length of the test cell and reference cell wires was 0.095 meter. From equation AI.46, the higher the thermal conductivity of a fluid, the greater the electrical heat input needed to raise the filament temperature any fixed amount. Water has the highest, and n-butanoic acid the lowest thermal conductivity of the fluids measured here. From calibration data, at approximately 361 F, a electrical potential of 3.555 volts in the filament with a resistance of 36.80 ohms was necessary to raise the temperature of the filament by 0.23 K. Using these values with the above equation for water yields:

$$\begin{aligned} Q_{el} &= ((3.555\ \text{V})^2/36.8\ \text{ohms}) * 0.5\ \text{s}/0.095\ \text{m} \\ &= 1.81\ \text{W/m} \end{aligned} \tag{AIII.6}$$

The radiant contribution of heat in the wire was only 0.021% at 450 K. At 73 F, from calibration data, an electrical potential of 2.765 volts for a wire with a resistance of 24.58 ohms was necessary to raise the temperature of the filament by 0.23 K. Using these values with equation AIII.5 for water yields:

$$\begin{aligned} Q_{el} &= ((2.765\ \text{V})^2/24.58\ \text{ohms}) * 0.5\ \text{s}/0.095\ \text{m} \\ &= 1.64\ \text{W/m} \end{aligned} \tag{AIII.7}$$

Dividing the maximum radiant heat flux by the electrically generated heat flux gives the ratio of radiation to conduction. The radiant contribution of heat in the wire for water at 73 F was only 0.0070%.

The same calculations can be done for n-butanoic acid, with the data taken from Table X. At 75 F, representative voltage and resistance values are: 1.699 volts and 24.67 ohms. At 308 F, representative values are: 2.058 volts and 34.62 ohms. At 75 F, the electrical heating was:

$$\begin{aligned} Q_{el} &= ((1.699\ \mathrm{V})^2/24.67\ \mathrm{ohms}) * 0.5\ \mathrm{s}/0.095\ \mathrm{m} \\ &= 0.62\ \mathrm{W/m} \end{aligned} \qquad \text{(AIII.8)}$$

At 308 F, the electrical heating was:

$$\begin{aligned} Q_{el} &= ((2.058\ \mathrm{V})^2/34.62\ \mathrm{ohms}) * 0.5\ \mathrm{s}/0.095\ \mathrm{m} \\ &= 0.64\ \mathrm{W/m} \end{aligned} \qquad \text{(AIII.9)}$$

Both values given above raised the wire temperature 0.23 K.

The maximum radiant contribution of heat transfer for each filament with n-butanoic acid was 0.018% and 0.052% at 75 and 308 F respectively, with a maximum radiant contribution of $3.31 * 10^{-4}$ W/m at 308 F (426.5 K), calculated from equation AIII.1.

Since water is not a transparent liquid, its true radiant contribution is found by multiplying the transparent radiant maximum by the infrared transmittance of water. The transmittance is found by subtracting the emissivity value from one. Water's average emissivity is 0.96, so its transmittance is 0.04. Therefore, the radiant contributions of water at 300 and 450 K are:

$$Q_{rad}\ (450\ K) = 3.88 * 10^{-4}\ W/m * 0.04$$
$$= 1.6 * 10^{-5}\ W/m \qquad (AIII.10)$$

and,

$$Q_{rad}\ (300\ K) = 1.15 * 10^{-4}\ W/m * 0.04$$
$$= 4.6 * 10^{-6}\ W/m \qquad (AIII.11)$$

The true radiant contributions are: 0.0009% and 0.0003% of the conduction heat transfer for water. The acids in this study are not transparent. Assuming a transmittance of 0.15 for the pure acids, which is conservative, the radiant contributions at 300 K and 426.5 K for n-butanoic acid would be:

$$Q_{rad}\ (300\ K) = 1.15 * 10^{-4}\ W/m * 0.15$$
$$= 1.7 * 10^{-5}\ W/m \qquad (AIII.12)$$

and,

$$Q_{rad}\ (426.5\ K) = 3.31 * 10^{-4}\ W/m * 0.15$$
$$= 5.0 * 10^{-5}\ W/m \qquad (AIII.13)$$

Good estimates for the true radiant contributions for the pure acids would be: 0.003% and 0.008% of the conduction heat transfer.

APPENDIX D

CALCULATIONS FOR MEASUREMENT ERROR SOURCES

Perfectly Cylindrical Filament

The filament radius in this work is 0.0013 cm. The time of measurement is 0.5 second. The thermal diffusivity of water at room temperature is approximately $1.44 * 10^{-3}$ cm^2/s, and the thermal diffusivity of n-butanoic acid at 300 F is approximately $6.6 * 10^{-4}$ cm^2/s Therefore, the following dimensionless factor ranges from 780 to 1700 for this apparatus.

$$G_0 = 4\alpha t/r^2 \qquad (AIV.1)$$

for water:

$$G_0 = 4 * 1.44 * 10^{-3}\ cm^2/s * 0.5\ s/(0.0013\ cm)$$
$$= 1700 \qquad (AIV.2)$$

for n-butanoic acid:

$$G_0 = 4 * 6.6 * 10^{-4}\ cm^2/s * 0.5\ s/\ (0.0013\ cm)$$
$$= 780 \qquad (AIV.3)$$

Expanding Temperature Gradient

The heat capacity and density of most liquids are in the range of 0.5 TO 1.0 BTU/# F and 0.5 to 1.5 gm/cm³, respectively. The measurement in this work generates from 0.6 to 1.8 watts. One watt-hour equals 3.414 BTU. One watt-second equals 0.000948 BTU.

$$0.6 \text{ W} * 0.5 \text{ s} * 0.000948 \text{ BTU/Ws} = 2.8 * 10^{-4} \text{ BTU} \qquad \text{(AIV.4)}$$

$$1.8 \text{ W} * 0.5 \text{ s} * 0.000948 \text{ BTU/Ws} = 8.5 * 10^{-4} \text{ BTU} \qquad \text{(AIV.5)}$$

To calculate the amount of fluid heated, a cylindrical geometry is used with a linear temperature gradient. Therefore, the average temperature change of the fluid is half the filament temperature change found for this work, or 0.12 K (0.2 F). The greatest volume of fluid is heated by a liquid of low heat capacity and density. Assuming a fluid with a heat capacity of 0.5 BTU/# F and density of 0.5 gm/cm³, and the highest heat input, the volume of heated fluid is approximately;

$$\text{Weight} = (1 \text{ \#F/0.5 BTU}) * 0.2 \text{ F} * (8.5 * 10^{-4} \text{ BTU}) = 0.00034 \text{ \#} \qquad \text{(AIV.6)}$$

$$\text{Volume} = (0.00034 \text{ \#}) * (454 \text{ gm/\#}) * (1 \text{ cm/0.5 gm}) = 0.31 \text{ cm}^3 \qquad \text{(AIV.7)}$$

The wire is 9.5 cm long. Disregarding the small radius and volume of the filament, the radial distance that the heat travels can be calculated from the following equation:

$$r = [(\mathrm{Volume}/\mathrm{Height}) / 3.14159]^{1/2} \qquad \text{(AIV.8)}$$

$$r = (0.31\ \mathrm{cm}^3/(9.5\ \mathrm{cm} / 3.14159))^{1/2}$$
$$= 0.10\ \mathrm{cm} = 1.0\ \mathrm{mm}$$

Coating on Wire

Nagasaka and Nagashima (51) state they had an uncertainty of 0.15% due to the coating on their wire. Their polyester coating thickness was 20% of the filament diameter. Their measurements lasted as long as 5 seconds. The coating thickness in this work is approximately 1% of the wire diameter (50). The time of the measurement was consistently 0.50 second. The relationship which shows the effect of the insulation on the thermal conductivity measurement is effectively:

$$\Delta^2 T = 1/t\ [\ln(r_1/r_0)]C_x \qquad \text{(AIV.9)}$$

where;

r_i = radius of insulated wire

$\Delta^2 T$ correction = correction to the temperature change slope

C_x = time and insulation independent terms

Therefore, for the relative error,

$$\text{Relative error} = (5/0.5) * \ln(1.01)/\ln(1.20) = 0.55 \quad (\text{AIV.10})$$

The uncertainty in the measurement caused by the presence of the coating is:

Uncertainty = 0.55 * 0.15% = 0.08%

Support Wire-Filament Junction

Irving and Jameison (33) have determined the potential error contributed to the measurement by the resistance of the support wire and the heat conducted into it during the measurement to be at most 3%. Their relationship of the error to the relative diameter if the filament and support wire is:

$$\text{Error} = C_a * (r^2/Ri^2) \quad (\text{AIV.11})$$

where;

C_a = a constant

R_i = radius of the support wire

r_o = radius of the filament

The radii of Irving and Jameison's filament and support wires (33) were; 0.00376 cm and 0.0190 cm, respectively. The radii of the filament and support wire in this work were: 0.0013 cm and 0.075 cm, respectively. The relative error of this work to that of Irving and Jameison is given by:

$$\text{Relative error} = [(0.0013 \text{ cm} * 0.0190 \text{ cm})/(0.00376 \text{ cm} * 0.075 \text{ cm})] = 0.0077 \quad \text{(AIV.12)}$$

The maximum error expected in this work as a result of support wire heating is:

$$\text{Error} = 3\% * 0.0077 = 0.023\%$$

APPENDIX E

THERMAL CONDUCTIVITY OF PURE AND AQUEOUS FORMIC, ACETIC, PROPIONIC, AND N-BUTANOIC ACIDS

TABLE IV

THERMAL CONDUCTIVITY OF AQUEOUS FORMIC ACID

T (F)	Vr	Vt	Rr	Rt	THERMAL CONDUCTIVITY (BTU/HR FT F)
FORMIC ACID CONCENTRATION					
76.0 MOL % (89.0 WT. %) -					
69.0	2.000	2.095	28.44	24.64	0.1614
139.7	2.000	2.241	28.44	27.75	0.1557
189.7	2.000	2.328	28.44	29.90	0.1504
247.5	2.000	2.420	28.44	32.33	0.1445
299.7	2.000	2.471	28.44	34.51	0.1350
40.21 MOL % (63.2 WT. %) -					
68.0	2.000	2.364	28.45	24.57	0.2333
130.4	2.000	2.505	28.45	27.34	0.2243
187.1	2.000	2.614	28.45	29.75	0.2152
233.1	2.000	2.732	28.45	31.71	0.2163
233.1	2.000	2.705	28.45	31.70	0.2100
262.3	2.000	2.771	28.45	32.91	0.2095
301.6	2.000	2.801	28.45	34.50	0.1969
19.86 MOL % (38.8 WT. %) -					
70.0	2.000	2.484	28.44	24.60	0.2699
124.6	2.000	2.636	28.45	26.97	0.2685
179.6	1.999	2.789	28.45	29.34	0.2688
227.0	1.999	2.900	28.45	31.34	0.2646
262.5	1.998	3.008	28.45	32.88	0.2685
302.1	2.000	3.073	28.45	34.52	0.2597
9.80 MOL % (21.74 WT. %) - SEE NOTE 1					
67.0	2.000	2.583	28.44	24.40	0.2898
131.8	2.000	2.796	28.44	27.15	0.2949
180.3	2.000	2.942	28.44	29.21	0.2987
229.5	2.000	3.051	28.44	31.28	0.2955
269.6	2.000	3.108	28.44	32.95	0.2874

TABLE IV CONTINUED

5.04 MOL % (11.9 WT. %) - SEE NOTE 2

68.0	1.999	2.542	28.44	24.41	0.3241
132.1	1.998	2.750	28.44	27.21	0.3355
182.9	2.000	2.943	28.44	29.43	0.3539
239.1	1.999	3.080	28.44	31.74	0.3531
286.1	2.000	3.172	28.44	33.70	0.3447

CALIBRATION CONSTANT IS 0.1054 UNLESS OTHERWISE NOTED

NOTE 1 - CALIBRATION CONSTANT =

$Co = 0.1015798 - 5.226093 * 10^{-5} *T(F) + 2.10647 * 10^{-7} *T^{2} (F)$

NOTE 2 - CALIBRATION CONSTANT =

$Co = 0.11474 + 2.29983 * 10^{-5} *T(F)$

TABLE V

THERMAL CONDUCTIVITY OF FORMIC ACID

AUTHOR	THERMAL CONDUCTIVITY AT 77 F (BTU/HR FT F)	TEMPERATURE RANGE (F)	TEMPERATURE COEFFICIENT $(BTU/HR/FT/F^2)$ $*10^3$
GUSEINOV	0.154	77 - 211	-0.028
FILIPPOV	0.158	59 - 194	-0.026
JOBST	0.129	-24 - 200	-0.154
POWELL	0.172 *	63	------
USMANOV	0.164 *	68	------
VARGAFTI	0.149 *	86	------
REIDEL	0.171 *	68	------
WEBER	0.157 *	77	------

* NOTE - ONLY ONE DATA POINT REPORTED

TABLE VI

THERMAL CONDUCTIVITY OF AQUEOUS ACETIC ACID

T (F)	Vr	Vt	Rr	Rt	THERMAL CONDUCTIVITY (BTU/HR FT F)
ACETIC ACID CONCENTRATION					
100 MOL % -					
68.0	2.000	1.756	28.43	24.41	0.09089
157.5	2.000	1.901	28.43	28.29	0.08548
202.6	2.000	1.960	28.44	30.20	0.08317
226.7	2.000	1.998	28.44	31.21	0.08325
226.7	2.000	1.992	28.44	31.21	0.08250
262.3	2.000	2.051	28.44	32.70	0.08345
304.7	2.000	2.092	28.44	34.47	0.08191
40.18 MOL % (69.13 WT. %) -					
78.0	2.000	2.050	28.43	24.43	0.1441
124.2	2.000	2.159	28.43	26.82	0.1390
177.7	2.000	2.288	28.43	29.10	0.1414
177.7	2.000	2.305	28.43	29.11	0.1445
225.7	2.000	2.421	28.43	31.14	0.1486
268.9	2.000	2.504	28.43	32.93	0.1502
300.6	2.000	2.546	28.44	34.26	0.1491
20.16 MOL % (45.70 WT. %) -					
67.0	2.000	2.285	28.44	24.37	0.2011
137.0	2.000	2.473	28.44	27.39	0.2005
193.0	2.000	2.612	28.44	29.73	0.2025
237.2	2.000	2.719	28.44	31.60	0.2056
268.5	2.000	2.781	28.44	32.92	0.2062
302.8	2.000	2.803	28.44	34.32	0.1986
10.06 MOL % (27.16 WT. %) -					
73.0	1.997	2.446	28.43	24.65	0.2417
125.6	2.000	2.612	28.43	26.93	0.2441
180.6	2.000	2.775	28.44	29.24	0.2502
231.2	2.000	2.898	28.44	31.38	0.2518
267.0	2.000	2.990	28.44	32.88	0.2601
302.5	2.000	3.046	28.44	34.34	0.2545

TABLE VI CONTINUED

5.05 MOL % (15.07 WT. %) -

71.0	2.000	2.583	28.44	24.58	0.2853
135.3	2.000	2.817	28.44	27.36	0.2970
164.6	2.000	2.913	28.44	28.66	0.3003
215.9	2.000	3.044	28.44	30.77	0.3016
254.9	2.000	3.132	28.44	32.36	0.3024
305.3	2.000	3.216	28.44	34.50	0.2974

NOTE: CALIBRATION CONSTANT =

$$Co = 0.1015798 - 5.226093 * 10^{-5} *T(F) + 2.10647 * 10^{-7} *T^{2}(F)$$

TABLE VII

THERMAL CONDUCTIVITY OF ACETIC ACID

AUTHOR	THERMAL CONDUCTIVITY AT 77 F (BTU/HR FT F)	TEMPERATURE RANGE (F)	TEMPERATURE COEFFICIENT (BTU/HR/FT/F^2) $*10^3$
THIS WORK	0.0915	68 - 305	-0.036
VENART	0.0920	63 - 174	-0.055
JOBST	0.0924	68 - 176	-0.064
FILIPPOV	0.0932	59 - 194	-0.062
VARGAFTIK	0.0989	77 - 167	-0.060
POWELL	0.0915 *	86	------
USMANOV	0.0976 *	68	------
JAMEISON	0.0907 *	77	------
FRONTASEV	0.0916 *	68	------
KERZHENTSEV	0.0979 *	77	------
VAN DE HELD	0.2244 *	73	------
FRONTASEV	0.1156 *	72	------
LEES	0.1040 *	77	------
WEBER	0.1141 *	54	------

* NOTE - DATA AVAILABLE AT ONLY ONE TEMPERATURE

TABLE VIII

THERMAL CONDUCTIVITY OF AQUEOUS PROPIONIC ACID

T (F)	Vr	Vt	Rr	Rt	THERMAL CONDUCTIVITY (BTU/HR FT F)
PROPIONIC ACID CONCENTRATION					
100 MOL % -					
72.0	2.004	1.729	28.43	24.55	0.08520
124.6	2.001	1.817	28.43	26.81	0.08279
190.8	2.000	1.921	28.44	29.71	0.08062
193.5	1.999	1.908	28.43	29.65	0.07943
262.0	2.000	2.019	28.44	32.60	0.08014
323.3	2.000	2.088	28.44	35.13	0.07956
40.23 MOL % (73.46 WT. %) -					
74.0	2.000	1.997	28.43	24.67	0.1307
140.9	1.989	2.124	28.43	27.56	0.1275
199.9	2.000	2.249	28.43	30.02	0.1270
252.9	2.000	2.339	28.43	32.27	0.1264
301.9	1.999	2.401	28.43	34.30	0.1250
20.13 MOL % (50.89 WT. %) -					
74.0	2.001	2.228	28.43	24.65	0.1815
131.1	2.000	2.346	28.44	26.86	0.1780
164.5	2.002	2.460	28.43	28.33	0.1844
178.9	2.000	2.478	28.44	28.92	0.1821
206.7	2.000	2.537	28.43	30.04	0.1824
232.4	2.000	2.609	28.44	31.18	0.1862
263.7	2.000	2.652	28.43	32.47	0.1831
302.3	2.000	2.711	28.44	34.11	0.1819
330.6	2.000	2.746	28.44	35.50	0.1783
10.29 MOL % (32.05 WT. %) -					
75.0	2.000	2.422	28.45	24.79	0.2312
75.0	2.000	2.415	28.44	24.71	0.2305
140.4	2.000	2.672	28.45	27.56	0.2500
182.5	2.000	2.805	28.46	29.37	0.2566

TABLE VIII CONTINUED

209.5	2.000	2.808	28.44	30.45	0.2411
251.6	2.000	2.885	28.46	32.21	0.2370
274.5	2.000	2.940	28.44	33.16	0.2385
274.5	2.000	2.923	28.44	33.04	0.2409
305.3	2.000	2.974	28.45	34.47	0.2358
5.41 MOL % (19.04 WT. %) -					
76.0	2.000	2.577	28.44	24.74	0.2793
136.1	2.000	2.800	28.43	27.33	0.2923
211.0	2.000	3.015	28.44	30.49	0.2976
271.1	2.000	3.145	28.44	33.01	0.2969
331.2	2.000	3.223	28.44	35.52	0.2881

CALIBRATION CONSTANT =

$$Co = 0.1015798 - 5.226093 * 10^{-5} *T(F) + 2.10647 * 10^{-7} *T^{2}(F)$$

TABLE IX

THERMAL CONDUCTIVITY OF PROPIONIC ACID

AUTHOR	THERMAL CONDUCTIVITY AT 77 F (BTU/HR FT F)	TEMPERATURE RANGE (F)	TEMPERATURE COEFFICIENT (BTU/HR/FT/F^2) $*10^3$
THIS WORK	0.0852	72 - 323	-0.021
MUKHAMEDZYANOV	0.0844	68 - 230	-0.035
JOBST	0.0855	32 - 334	-0.039
POWELL	0.0887 *	86	------
WEBER	0.0944 *	54	------

* NOTE - ONLY ONE DATA POINT REPORTED

TABLE X

THERMAL CONDUCTIVITY OF AQUEOUS N-BUTANOIC ACID

T (F)	Vr	Vt	Rr	Rt	THERMAL CONDUCTIVITY (BTU/HR FT F)
N-BUTANOIC ACID CONCENTRATION					
100 MOL % -					
75.0	2.000	1.699	28.44	24.67	0.08053
75.0	2.000	1.743	28.44	24.74	0.08646
161.8	2.000	1.877	28.44	28.41	0.08171
233.4	2.000	1.977	28.44	31.45	0.07967
308.8	2.000	2.058	28.44	34.62	0.07760
49.06 MOL % (82.50 WT. %) -					
72.0	2.000	1.958	28.41	24.25	0.1170 (3)
97.9	2.000	2.004	28.41	25.35	0.1148 (3)
153.7	2.000	2.137	28.41	27.81	0.1157 (3)
202.3	2.000	2.094	28.41	30.04	0.1078 (1)
202.3	2.000	2.106	28.41	30.05	0.1096 (1)
215.9	2.000	2.244	28.41	30.41	0.1120 (3)
284.8	2.000	2.272	28.42	33.25	0.1063 (3)
333.7	2.000	2.255	28.41	35.37	0.09709 (1)
24.92 MOL % (61.89 WT. %) -					
77.0	2.000	2.124	28.41	24.73	0.1562
219.0	2.000	2.418	28.41	30.14	0.1573
287.8	2.000	2.519	28.41	33.05	0.1536
355.8	2.000	2.601	28.41	36.46	0.1465
10.15 MOL % (35.64 WT. %) -					
75.0	2.000	2.430	28.42	24.43	0.2427 (2)
118.9	2.000	2.553	28.42	26.34	0.2422 (2)
188.7	2.000	2.742	28.42	29.32	0.2422 (2)
201.8	2.000	2.742	28.41	29.94	0.2436 (1)
264.1	2.000	2.849	28.41	32.54	0.2314 (1)
265.0	2.000	2.895	28.43	32.48	0.2324 (2)
319.3	2.000	2.958	28.41	34.82	0.2261 (1)

TABLE X CONTINUED

5.00 MOL % (20.47 WT. %) -

76.0	1.997	2.555	28.44	24.78	0.2740
139.6	2.000	2.774	28.44	27.52	0.2804
167.5	2.000	2.863	28.43	28.72	0.2838
184.6	2.000	2.918	28.44	29.40	0.2880
211.1	2.000	2.978	28.43	30.47	0.2872
230.6	2.000	3.020	28.44	31.34	0.2856
292.6	2.000	3.155	28.44	33.95	0.2874
329.1	2.000	3.169	28.44	35.40	0.2752

CALIBRATION CONSTANT =

$Co = 0.1015798 - 5.226093 * 10^{-5} *T(F) + 2.10647 * 10^{-7} *T^{2} (F)$

NOTE 1 - CALIBRATION CONSTANT IS 0.1054

NOTE 2 - CALIBRATION CONSTANT IS 0.1001

NOTE 3 - CALIBRATION CONSTANT IS 0.09088

TABLE XI

THERMAL CONDUCTIVITY OF N-BUTANOIC ACID

AUTHOR	THERMAL CONDUCTIVITY AT 77 F (BTU/HR FT F)	TEMPERATURE RANGE (F)	TEMPERATURE COEFFICIENT (BTU/HR/FT/F^2) $*10^3$
THIS WORK	0.0851	75 - 309	-0.024
MUKHAMEDZYANOV	0.0824	68 - 320	-0.039
JOBST	0.0853	32 - 338	-0.057
POWELL	0.0861	86	------
USMANOV	0.0849	68	------
FILIPPOV	0.0861	86	------
SKRYNNIKOVA	0.0866	86	------
WEBER	0.0871	54	------

* NOTE - ONLY ONE DATA POINT REPORTED

APPENDIX F

HEAT CAPACITY, DENSITY, THERMAL CONDUCTIVITY AND THERMAL DIFFUSIVITY DATA FOR SELECT COMPOUNDS

TABLE XII

THERMAL CONDUCTIVITY OF SELECTED COMPOUNDS

T(C)	WATER (35)	N-BUTANOIC ACID (THIS WORK)	GLYCEROL (35)	PENTANE (35)	TOLUENE (35)
20	0.3485	0.0853	0.1648	0.0676	0.0758
30	0.3568	0.0849	0.1653	0.0656	0.0742
40	0.3644	0.0845	0.1657	0.0636	0.0727
50	0.3712	0.0840	0.1662	0.0616	0.0711
60	0.3771	0.0836	0.1666	0.0597	0.0696
70	0.3823	0.0832	0.1671	0.0577	0.0681
80	0.3868	0.0827	0.1676	0.0557	0.0667
90	0.3904	0.0823	0.1680	0.0537	0.0653
100	0.3933	0.0819	0.1685	0.0517	0.0639
110	0.3955	0.0814	0.1689	0.0497	0.0626
120	0.3970	0.0810	0.1694	------	0.0613
130	0.3977	0.0806	0.1699	------	0.0601
140	0.3978	0.0801	0.1703	------	0.0589
150	0.3971	0.0797	0.1708	------	0.0577
160	0.3958	------	------	------	0.0565
170	0.3939	------	------	------	0.0554
180	0.3912	------	------	------	0.0543
190	0.3880	------	------	------	0.0533
200	0.3841	------	------	------	0.0523

NOTE - ALL VALUES REPORTED IN BTU/HR FT F

TABLE XIII

HEAT CAPACITY OF SELECTED COMPOUNDS

T(C)	WATER (76)	N-BUTANOIC ACID (16)	GLYCEROL (76)	PENTANE (76)	TOLUENE (76)
0	4.218	1.950	-----	2.218	1.639
10	4.194	1.985	2.288	2.268	1.669
20	4.182	2.020	2.345	2.318	1.700
30	4.179	2.056	2.401	2.393	1.733
40	4.179	2.091	2.457	2.469	1.766
50	4.181	2.126	2.513	2.560	1.800
60	4.185	2.161	2.568	2.652	1.834
70	4.191	2.196	2.624	2.741	1.868
80	4.198	2.232	2.678	2.866	1.903
90	4.207	2.267	2.733	2.971	1.937
100	4.218	2.302	2.788	3.117	1.971
110	4.230	2.337	2.842	-----	2.005
120	4.244	2.373	2.896	-----	2.037
130	4.262	2.408	2.950	-----	2.069
140	4.282	2.443	3.004	-----	2.100
150	4.306	2.478	3.058	-----	2.134
160	4.334	2.513	3.112	-----	2.166
170	4.366	2.549	3.165	-----	-----
180	4.403	2.584	3.219	-----	-----
190	4.446	2.619	3.273	-----	-----
200	4.494	2.654	3.327	-----	-----

NOTE - ALL VALUES REPORTED IN KJ/KG C

TABLE XIV

DENSITY OF SELECTED COMPOUNDS

T(C)	WATER (44)	N-BUTANOIC ACID (44)	GLYCEROL (44)	PENTANE (44)	TOLUENE (44)
0	0.9999	0.9739	1.2751	0.6577	0.8915
10	0.9997	0.9647	1.2688	0.6469	0.8822
20	0.9982	0.9555	1.2625	0.6362	0.8729
30	0.9957	0.9463	1.2562	0.6254	0.8636
40	0.9923	0.9371	1.2499	0.6147	0.8544
50	0.9881	0.9279	1.2436	0.6039	0.8451
60	0.9832	0.9187	1.2373	0.5932	0.8358
70	0.9778	0.9096	1.2310	0.5825	0.8265
80	0.9718	0.9004	1.2247	0.5717	0.8172
90	0.9653	0.8912	1.2183	0.5610	0.8079
100	0.9584	0.8820	1.2120	0.5502	0.7987
110	0.9510	0.8728	1.2057	0.5395	0.7894
120	0.9434	0.8636	1.1994	0.5287	0.7801
130	0.9352	0.8544	1.1931	0.5180	0.7708
140	0.9264	0.8452	1.1868	0.5073	0.7615
150	0.9173	0.8360	1.1805	0.4965	0.7523
160	0.9075	0.8268	1.1742	-----	0.7430
170	0.8973	0.8176	1.1678	-----	0.7337
180	0.8866	0.8084	1.1616	-----	0.7244
190	0.8750	0.7992	1.1553	-----	0.7151
200	0.8628	0.7900	1.1489	-----	0.7058

NOTE - ALL VALUES REPORTED IN g/cm^3

TABLE XV

THERMAL DIFFUSIVITY OF SELECTED COMPOUNDS

T (C)	WATER	N-BUTANOIC ACID	GLYCEROL	PENTANE	TOLUENE
20	1.44	0.765	0.963	0.793	0.885
30	1.48	0.755	0.949	0.759	0.858
40	1.48	0.746	0.934	0.725	0.833
50	1.52	0.737	0.920	0.690	0.809
60	1.54	0.721	0.907	0.657	0.786
70	1.56	0.712	0.895	0.625	0.742
80	1.62	0.705	0.884	0.588	0.722
90	1.64	0.698	0.873	0.558	0.703
100	1.66	0.691	0.863	0.522	0.685
110	1.68	0.684	0.853	-----	0.668
120	1.72	0.678	0.844	-----	0.652
130	1.73	0.671	0.835	-----	0.637
140	1.74	0.666	0.827	-----	0.622
150	1.74	0.661	0.819	-----	0.608

* NOTE - ALL VALUES REPORTED IN (10^3) cm^2/s

VITA 2

Edward R. Peterson

Candidate for the Degree of

Doctor of Philosophy

Thesis: MEASUREMENT OF THERMAL CONDUCTIVITY OF AQUEOUS ORGANIC LIQUIDS USING THE RELATIVE TRANSIENT HOT-WIRE TECHNIQUE

Major Field: Chemical Engineering

Biographical:

Personal Data: Born in Marion, New York, September 23, 1956, the son of Clinton and Audrey Peterson; married to Janet E. Suhay on July 22, 1978.

Education: Graduated from Marion Central High in June 1974; B.S. in Chemistry from Houghton, N.Y., in 1978; M.S. in Chemical Engineering from Rice University, Texas, in 1981; completed requirements for the Doctor of Philosophy Degree in July, 1985, at Oklahoma State University.

Professional Experience: Employed by Conoco Chemicals Research in Ponca City, Oklahoma, from June, 1980, until August, 1982. Held the position of Engineer in the Department of Engineering Research. Major duties encompassed all design, development, and construction responsibilities for High Density Polyethylene pilot plant.

Membership: American Chemical Society, American Institute of Chemical Engineers, National Society of Petroleum Engineers.

Professional Status: Registered as an Engineering Intern in Oklahoma since July, 1981 (# 5173).